



Calhoun: The NPS Institutional Archive

Theses and Dissertations

Thesis Collection

1991-03

Mesoscale variability of the Caribbean Sea from GEOSAT

Andrade Amaya, Carlos Alberto

Monterey, California. Naval Postgraduate School

<http://hdl.handle.net/10945/28353>



Calhoun is a project of the Dudley Knox Library at NPS, furthering the precepts and goals of open government and government transparency. All information contained herein has been approved for release by the NPS Public Affairs Officer.

Dudley Knox Library / Naval Postgraduate School
411 Dyer Road / 1 University Circle
Monterey, California USA 93943

<http://www.nps.edu/library>

NAVAL POSTGRADUATE SCHOOL

Monterey, California



THESIS

A4892

MESOSCALE VARIABILITY OF THE CARIBBEAN SEA
FROM GEOSAT

by

Carlos Alberto Andrade Amaya

March 1991

Thesis Advisor:
Co-Advisor:

Jeffrey A. Nystuen
Carlyle H. Wash

Approved for public release; distribution is unlimited

T254016
T254017

REPORT DOCUMENTATION PAGE

1a. REPORT SECURITY CLASSIFICATION Unclassified			1b. RESTRICTIVE MARKINGS		
2a. SECURITY CLASSIFICATION AUTHORITY			3. DISTRIBUTION/AVAILABILITY OF REPORT Approved for public release; distribution is unlimited		
2b. DECLASSIFICATION/DOWNGRADING SCHEDULE					
4. PERFORMING ORGANIZATION REPORT NUMBER(S)			5. MONITORING ORGANIZATION REPORT NUMBER(S)		
6a. NAME OF PERFORMING ORGANIZATION Naval Postgraduate School		6b. OFFICE SYMBOL (If applicable)	7a. NAME OF MONITORING ORGANIZATION Naval Postgraduate School		
6c. ADDRESS (City, State, and ZIP Code) Monterey, CA 93943-5000			7b. ADDRESS (City, State, and ZIP Code) Monterey, CA 93943-5000		
8a. NAME OF FUNDING/SPONSORING ORGANIZATION		8b. OFFICE SYMBOL (If applicable)	9. PROCUREMENT INSTRUMENT IDENTIFICATION NUMBER		
8c. ADDRESS (City, State, and ZIP Code)			10. SOURCE OF FUNDING NUMBERS		
			Program Element No.	Project No.	Task No.
					Work Unit Accession Number
11. TITLE (Include Security Classification) MESOSCALE VARIABILITY OF THE CARIBBEAN SEA FROM GEOSAT (U)					
12. PERSONAL AUTHOR(S) CARLOS ALBERTO ANDRADE AMAYA					
13a. TYPE OF REPORT Master's Thesis		13b. TIME COVERED From To		14. DATE OF REPORT (year, month, day) March 1991	
				15. PAGE COUNT 55	
16. SUPPLEMENTARY NOTATION					
17. COSATI CODES			18. SUBJECT TERMS (continue on reverse if necessary and identify by block number)		
FIELD	GROUP	SUBGROUP	GEOSAT , CARIBBEAN SEA , OCEANOGRAPHY , WIND STRESS, WIND SPEED ,		
			SEA SURFACE MESOSCALE VARIABILITY		
19. ABSTRACT (continue on reverse if necessary and identify by block number)					
<p>Two years of GEOSAT Exact Repeat Mission (ERM) altimetry and wind speed measurements in the Caribbean Sea are used to determine the sea surface height mesoscale variability and to characterize the wind stress field during 1987-88. The along track sea surface anomalies are determined using alongtrack derivatives for the estimation of the mean sea surface height and a least square fit is used to remove the orbital error. Biased points near land were removed and high frequency noise was filtered by using a 70 km spatial running mean. Contours of sea surface height anomalies made by every ERM period detected the formation and evolution of two anticyclonic eddies formed during the "non-windy" tropical season, one each year, with a height signature that reached +30 cm. No eddies related to the Caribbean Current were apparent during the other seasons. A quasi-permanent cyclonic eddy was detected near the San Andres Archipelago, confirming model predictions. Seasonal wind speed derived from GEOSAT data agrees with previous studies in the area. The relaxation of the wind after the "windy" season and the strong meridional wind stress gradient in the center of the Caribbean coincide with the formation of the anticyclones. This suggests that the wind field influences eddy formation. Anomalies in the averaged wind field were produced by strong synoptic events (hurricanes) which are biased due to the 17 day sampling character of the GEOSAT data.</p>					
20. DISTRIBUTION/AVAILABILITY OF ABSTRACT <input checked="" type="checkbox"/> UNCLASSIFIED/UNLIMITED <input type="checkbox"/> SAME AS REPORT <input type="checkbox"/> DTIC USERS			21. ABSTRACT SECURITY CLASSIFICATION Unclassified		
22a. NAME OF RESPONSIBLE INDIVIDUAL Jeffrey A. Nystuen			22b. TELEPHONE (Include Area code) (408) 646 - 2917		22c. OFFICE SYMBOL Oc / Ny

Approved for public release; distribution is unlimited.

Mesoscale Variability of the Caribbean Sea from GEOSAT

by

Carlos Alberto Andrade Amaya
Lieutenant Commander, Colombian Navy
B.S., Colombian Naval Academy

Submitted in partial fulfillment
of the requirements for the degrees of

MASTER OF SCIENCE IN PHYSICAL OCEANOGRAPHY
and
MASTER OF SCIENCE IN METEOROLOGY

from the

ABSTRACT

Two years of GEOSAT Exact Repeat Mission (ERM) altimetry and wind speed measurements in the Caribbean Sea are used to determine the sea surface height mesoscale variability and to characterize the wind stress field during 1987-88. The alongtrack sea surface anomalies are determined using alongtrack derivatives for the estimation of the mean sea surface height and a least square fit is used to remove the orbital error. Biased points near land were removed and high frequency noise was filtered by using a 70 km spatial running mean. Contours of sea surface height anomalies made by every ERM period detected the formation and evolution of two anticyclonic eddies formed during the "non-windy" tropical season, one each year, with a height signature that reached + 30 cm. No eddies related to the Caribbean Current were apparent during the other seasons. A quasi-permanent cyclonic eddy was detected near the San Andres Archipelago, confirming model predictions. Seasonal wind speed derived from GEOSAT data agrees with previous studies in the area. The relaxation of the wind after the windy season and the strong meridional wind gradient in the center of the Caribbean coincide with the formation of the anticyclones. This suggests that the wind field influences eddy formation. Anomalies in the averaged wind field were produced by strong synoptic events (hurricanes) which are biased due to the 17 day sampling character of the GEOSAT data.

180513
H4622
C.1

TABLE OF CONTENTS

I. INTRODUCTION	1
II. BACKGROUND	3
A. BASIN DESCRIPTION	3
B. METEOROLOGY BACKGROUND	10
C. THEORETICAL BACKGROUND	12
III. METHODOLOGY	17
A. HEIGHT CORRECTIONS	17
B. WIND SPEED CALCULATION	25
IV. RESULTS	27
A. HEIGHT ANOMALY ANALYSIS	27
B. WIND ANALYSIS	37
C. DISCUSSION OF THE RESULTS	42
V. CONCLUSIONS	47

LIST OF REFERENCES	49
--------------------------	----

INITIAL DISTRIBUTION LIST	55
---------------------------------	----

LIST OF FIGURES

Figure 1 Caribbean Sea bottom topography and general circulation (from Molinari,1981).	4
Figure 2 Trajectories of drifting buoys in the Caribbean (from Molinari et al.,1981)	9
Figure 3 Surface currents in the western Caribbean (from Gordon, 1990)	10
Figure 4 Wind regime in the Caribbean (from Pujos et al.,1986)	11
Figure 5 Raw data from orbit 2843 A (an ascending orbit with equatorial crossing at 284.3°E or 75.7°W).	18
Figure 6 Mean sea level for GEOSAT Orbit 2843 A	21
Figure 7 Heights after demeaning process GEOSAT Orbit 2843A	22
Figure 8 Heights after orbital removal (shifted 50 cm).	23
Figure 9 Heights after smoothing process GEOSAT orbit 2843A	24
Figure 10 GEOSAT orbit tracks over the Caribbean Sea	24
Figure 11 GEOSAT detection	27
Figure 12 Mesoscale variability 14 May 1987 contour interval is 10 cm.	28

Figure 13 Mesoscale variability 31 May 1987	
contour interval is 10 cm.	29
Figure 14 Mesoscale variability 17 June 1987	30
Figure 15 Mesoscale variability 4 July 1987	30
Figure 16 Mesoscale variability 21 July 1987	
contour interval is 10 cm.	31
Figure 17 Mesoscale variability 13 April 1988	
contour interval is 10 cm.	32
Figure 18 Mesoscale variability 30 April 1988	33
Figure 19 Mesoscale variability 17 May 1988	33
Figure 20 Mesoscale variability 30 September 1988	34
Figure 21 Mesoscale variability 3 November 1988	34
Figure 22 Collinear tracks Orbit 2791 D (a descending orbit with equatorial crossing at $279.1^{\circ}\text{E} = 80.9^{\circ}\text{W}$)	35
Figure 23 Time series of the height anomalies for Orbit B in Figure 6.	36
Figure 24 Root Mean Square variability during 1987-88 (cm)	
contour interval is 1 cm.	37
Figure 25 Wind Speed in the Caribbean during 1987-88.	38
Figure 26 Wind Speed March-May 1987 (contour interval 1 m/s)	39
Figure 27 Wind Speed May-Sept 1987 (contour interval 1 m/s)	39
Figure 28 Wind Speed Sept-Nov 1987 (contour interval 1 m/s)	40
Figure 29 Wind Speed during November/87 - March/88 (m/s)	41

Figure 30 Wind Speed Mar-June 1988 (contour interval 1 m/s)	41
Figure 31 Hurricanes in the Caribbean in 1987 (Case, 1988)	43
Figure 32 Hurricanes during 1988 (Gross et al., 1989)	43
Figure 33 Wind speed Jun-Sep 1988 (contour interval 1 m/s)	44
Figure 34 Wind Speed Sept-Nov 1988 (contour interval 1 m/s)	44

ACKNOWLEDGMENTS

My first thanks goes to the Jet Propulsion Lab who provided the GEOSAT data, that made this work possible. Most helpful was Elizabeth Smith who assisted with the conversion of UNIX format into a more generic ASCII code.

I would like to express my sincere thanks to the Faculty of the Departments of Oceanography and Meteorology for the knowledge offered to me during these two years, especially to Dr. Curtis Collins, for his vote of confidence and support during the difficult moments of academic life.

I would also like to thank my advisors Professors Jeffrey Nystuen and Carlyle Wash for showing me the exciting and challenging field of remote sensing. They were a constant source of encouragement and enlightenment. They have allowed me to experience the thrill and satisfaction that results from scientific inquiry. Their hours of patient, especially with my written english, counsel, and guidance enabled me to form and express the concepts herein. Without their guidance and assistance none of this would have been possible.

My acknowledgement would not be complete without recognizing Arlene Bird, Donna Burych and the staff at the IDEA Lab, for their assistance with the code used for the heights and wind speed calculations.

The support and friendship of the U.S. Navy and officers of other countries was invaluable in accomplish this task. I feel myself fortunate to have meet them and I want to thank them all.

Finally, I would like to thank my wife, Margarita for her enduring support, love and understanding during the course of these challenging pursuits; to my children Carlos and Kristina that one day will understand why their Dad couldn't share enough time with them for these two years; and to the Good Lord for sharing the wonders of his creation.

I. INTRODUCTION

The oceanography of the Caribbean Sea is of great importance because it is known to play a fundamental role in the Gulf Stream System formation and consequently affects the circulation of the North Atlantic Ocean (Anderson and Corry, 1985). Its waters are rich in temporal and spatial scales of variability, e.g. Molinari et al.(1981). The complexity of the near surface dynamics affects formation, dissipation (eddy) dynamics and coastal upwelling (Maul, 1988). Modern understanding of the surface currents in the Caribbean Sea is based on studies that have concentrated on shipboard measurements of dynamic topography, e.g. Gordon (1967), and Morrison and Nowlin (1982).

In the past decade satellite altimeters have demonstrated the ability to detect dynamic ocean features. Satellite altimetry from GEOS-3 and SEASAT have shown sea surface height variability of ± 20 cm in the Caribbean (Douglas et al., 1983; Marsh et al., 1984). The most recent radar altimeter, carried by GEOSAT, has detected ocean features with spatial scales of order 50 km, e.g. Leben et al.,(1990) and with dynamic height anomalies of ± 10 cm.

The present study is undertaken as a step toward the observation of the mesoscale variability of the sea surface as well as the characterization of the wind speed field in the Caribbean Sea using GEOSAT altimetry data. Special attention will be focused on the Western Caribbean because most of the work until now

has been done in the eastern part of this basin and very little is known about the vast western zone. Previous studies, e.g. Molinari et al. (1981), have suggested that the circulation in this area is governed principally by mesoscale features and the expectation is that GEOSAT resolution will be high enough to detect such features.

II. BACKGROUND

A. BASIN DESCRIPTION

The Caribbean Sea is a semi-enclosed basin in of the western North Atlantic Ocean. It is limited on the south by South America, on the west by Central America from Venezuela to the Yucatan Peninsula, on the east by the Lesser Antilles and in the north by the Greater Antilles. This complicated geography suggest extensive variability and complexity which should make the Caribbean an exciting and intriguing focus of study.

Using bottom topography, the Caribbean Basin can be divided into different regions as is shown in Fig. 1. From right to left, the Granada Basin is between the Lesser Antilles arc and the Aves Ridge, the Venezuela Basin and the Colombian Basin are separated by the Beata Rise. Between the Colombia Basin and the Cayman Basin is the Jamaica Ridge which extends to the south-west forming the Nicaraguan Rise. Finally, farther north, the Yucatan Basin is separated from the Cayman Basin by the Cayman Ridge and ends in the Yucatan Strait.

The oceanography of the Caribbean Sea has been subject of scientific investigation since last century. Among the first studies published are general descriptions of the oceanography of the basin by Parr (1927) and Dietrich (1939). Wust(1963) and Worthington (1955,1966) discuss the water structure of the Caribbean especially for the deep layers. In these studies it was shown that the

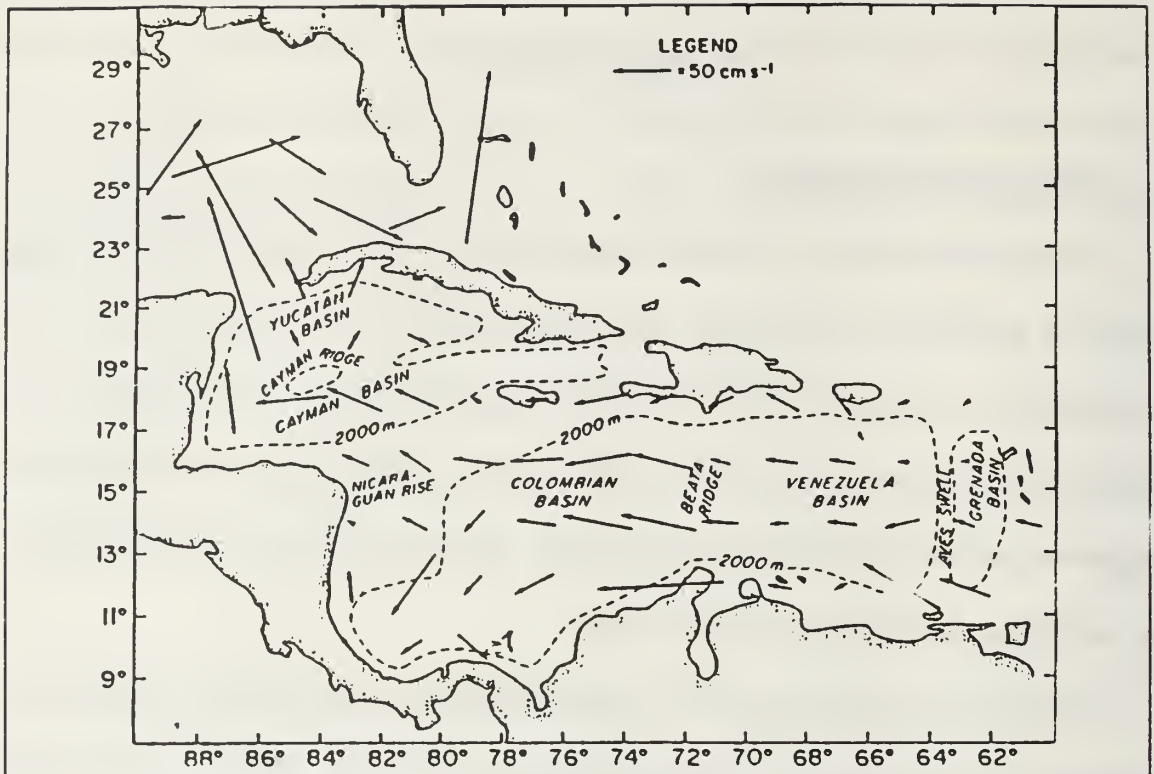


Figure 1 Caribbean Sea bottom topography and general circulation (from Molinari, 1981).

water structure is principally controlled by the sill depths between the island arcs. Thus, the Caribbean is highly stratified in the upper 1000 m, weakly stratified to 2000 m and nearly homogeneous below 2000 m. Morrison and Nowlin (1982) described the distribution of water masses in the eastern Caribbean Sea. In particular, Subtropical Underwater enters the Caribbean through the Lesser Antilles; Sargasso Sea Water enters through the Greater Antilles; Tropical Atlantic Central Water and Antarctic Intermediate Water enter through the southern Lesser Antilles and North Atlantic Deep Water enters the Venezuelan Basin through the Anegada Passage and the Colombian Basin through the channel between Jamaica and Hispaniola. Aguilera and Andrade (1989) verified the

presence of 18°C Sargasso Sea Water, Tropical Atlantic Central Water and Antarctic Intermediate Water near the San Andres Archipelago (Lat 13°N - Long 83°W).

The dynamics of the deep water is discussed in several works. Wust (1963) presented an analysis made from data collected during 30 oceanographic cruises to describe the deep water circulation. It is known that the deep and bottom waters within the Caribbean are renewed principally through the passages in the Greater Antilles (Windward and Anegada Passages), although the nature of the bottom water renewal is controversial, see e.g. Sturges (1965), Dietrich (1939), Wust (1964) and Froelich and Atwood (1974). Worthington (1955,1966) suggested that no renewal of the bottom water has occurred in recent times and that a slow warming of the Caribbean bottom water is occurring. This statement was supported by Richards and Vaccaro (1956) who found anaerobic conditions in the Cariaco Trench (north of Trinidad). More recently, Atwood et al. (1979) showed that renewal processes are still occurring from measurements of the deep silicate content in the same area. Hansen and Molinari (1979) detected deep currents (15 meters above the bottom) in the Yucatan Strait that are generally southward. This suggests water inflow into the Yucatan Basin of the north Caribbean Sea.

The general orientation of the surface currents and wind direction in the Caribbean is east to west. This wind orientation is believed to be responsible for upwelling which has been reported by several authors near the coast of Colombia and Venezuela. Gordon (1967) and Fajardo (1979) discussed some physical

features of the upwelling, and Corredor (1979) described how the growth rate of phytoplankton in these areas is significantly slower compared to other upwelling sites due to the impoverished Subtropical Underwater origin of the upwelling water.

Richards (1960) described the chemical characteristics in the East Caribbean verifying that upwelling exists off the northern South American coast. He also described particular chemical features of the Cariaco Trench. Froelich et al.(1978) showed that the Amazon River is responsible for as much as 60% of the total variability of surface salinity and dissolved silicate concentration of the Eastern Caribbean.

Analysis of tidal characteristics in the Caribbean Sea has shown that this basin has a microtidal range. Mofjeld and Winbush (1977) showed that the theory of cotidal charts could be verified in the Caribbean using bottom pressure variation measurements. Kjerfve (1981) made a complete study of the tidal behavior in the Caribbean using 45 tide gauges around the basin. He concluded that the tide is primarily either mixed semidiurnal or mixed diurnal with amplitudes of about 10 cm. He also stated that there is a strong radiational forcing of the S2 tide in the southwestern Caribbean but with an average amplitude of only 3.3 cm. Finally he commented that due to the small magnitude of the forcing, synoptic meteorological or oceanographic conditions may, at times, entirely mask the tidal response. Mofjeld and Winbush (1977) noted that atmospheric waves of 4-5 days periods produced by easterly winds are relatively

significant when compared with the amplitude of the tides in the area.

Wust (1963) made the first attempt to describe the surface dynamics using long term averages of extensive ship drift observations to represent the mean monthly surface currents. In general, the main feature of the surface circulation in the Caribbean is the Caribbean Current, which lies along the main east-west axis of the sea. This current is a continuation of the North Atlantic Countercurrent and/or the Guyana Current which reach to the Lesser Antilles. The Caribbean Current flows to the west through the basin and passes through the Yucatan Strait into the Gulf of Mexico. This water eventually reaches the Florida Strait and forms part of the Gulf Stream. The contribution of the Caribbean Current to the volume transport of the Gulf Stream is important because variations within the basin, such as due to wind stress, may result in significant changes in the stability and behavior of the Gulf Stream (Maul 1988).

Gordon (1967) described upper layer circulation of the Caribbean Sea using six north-south hydrographic profiles across the basin. He described the axis of the Caribbean Current using the classical geostrophic method. His calculation of the volume transport was 31 Sv toward the west. Maps of surface dynamic topography from that work show gyres in the western Caribbean and suggest the presence of a countercurrent along Costa Rica and Panama which ends on the Colombian coast. This flow is usually called the Darien Countercurrent. This recirculation flow is also shown in Wust (1964).

Roemich (1981) used an inverse method to make a calculation of the

geostrophic flow by imposing mass and salt conservation. The method showed an ability in resolve large features of the circulation, and, in principal, described how the flow seems to separate into several streams and eddies in the Venezuela Basin. It becomes a broad current in the southern part in the Colombian Basin and suggests the presence of a recirculation flow near Jamaica. The profiles also showed that the entire basin has a cyclonic circulation in the deep waters. He calculated the total transport leaving the basin to be 29 Sv, made up of 22 Sv from the east flowing across the Caribbean and 7 Sv entering from Windward Passage into the north Cayman basin.

Molinari et. al. (1981) observed the surface currents using Lagranian drifting buoys deployed near the Lesser Antilles. The results of this work showed zones of intense mesoscale variability, especially over the Aves Rise, Beata Ridge and the Nicaraguan Rise, (Fig. 2). Large eddies and meanders near these areas suggest that the rises and ridges of the Caribbean Sea may be an important source of the mesoscale variability in the basin. The study also showed how the Caribbean Current intensifies off the coast of Colombia, south of the Nicaraguan Rise and south of the Yucatan Strait.

The influence of the Darien Countercurrent on the continental shelf circulation and its action on the dispersion of sediments in suspension from the Magdalena River (Colombia) was studied during the "Caracolante" cruises and published in Pujos et al., (1986). This work showed that the intensity of the Darien Countercurrent varies seasonally reaching the Guajira Peninsula (72° W) in

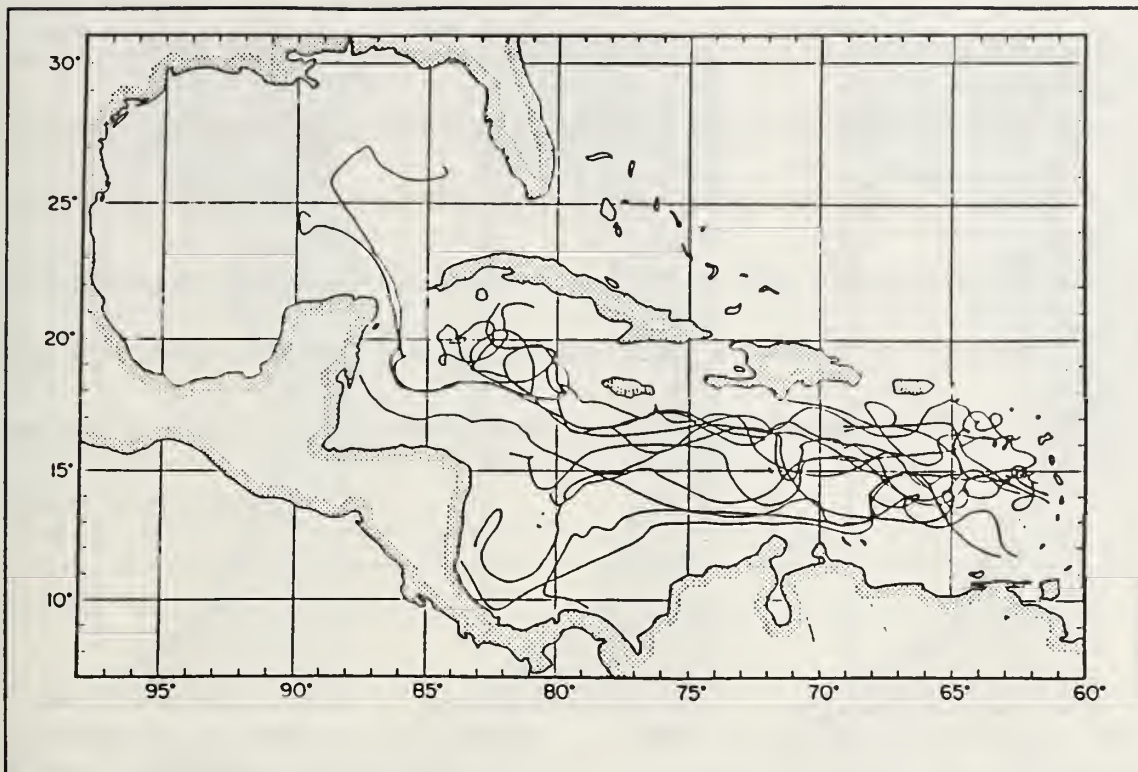


Figure 2 Trajectories of drifting buoys in the Caribbean
(from Molinari et al., 1981)

October-November and retracting its effect to the Darien Gulf (77° W) during February-March. The study also showed several cyclonic eddies near Cartagena, Colombia (76° W) which were attributed to the influence of this Countercurrent.

L. Gordon (pers. commun., 1990), as a collateral result of a long term run of the global eddy resolving model, the so called "Semtner Model" observed an eddy off the Costa Rican coast. The eddy showed a strong seasonal intensification in Nov-Feb and disappeared in June-July, Fig. 3.

A primitive equation model of the sea surface dynamic height in the Caribbean Sea by Thompson (pers. commun., 1990) verified most of the large features of the circulation described here. It also indicated a well established

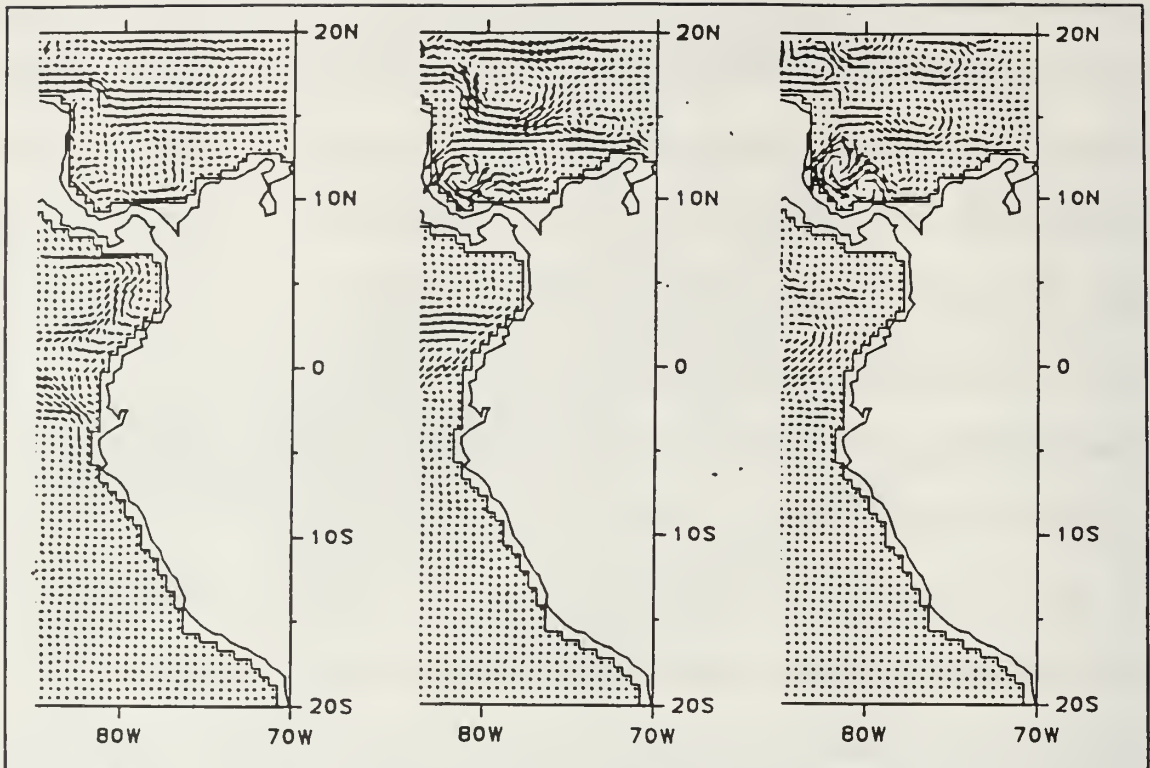


Figure 3 Surface currents in the western Caribbean
(from Gordon, 1990)

cyclonic eddy centered at 11° N, 82° W off the coast of Costa Rica which showed seasonal variation.

B. METEOROLOGY BACKGROUND

The climate of the Caribbean basin is characterized by two tropical "seasons": a dry or windy season from November to March and a humid or rainy season from July to September. The rest of the year is considered to be transition between these stages (Pujos et al., 1986).

This climate pattern is modulated by the presence of the Intertropical Convergence Zone (ITCZ). Sadler (1967) stated that during August the main trough of the ITCZ is located in the Northern Hemisphere over the Caribbean. In

areas where this trough is displaced poleward more than about 10° N, as is in the Caribbean, the trade winds crossing the equator from the Southern Hemisphere acquire a westerly component. This leads to a cyclonic shear zone across the ITCZ which serves as a genesis area for tropical vortices (Fig. 4 May-Sep, Pujos et al. 1986). This shear zone over the Central and South American land mass results in a favorable location for synoptic and mesoscale disturbances which normally produce heavy precipitation.

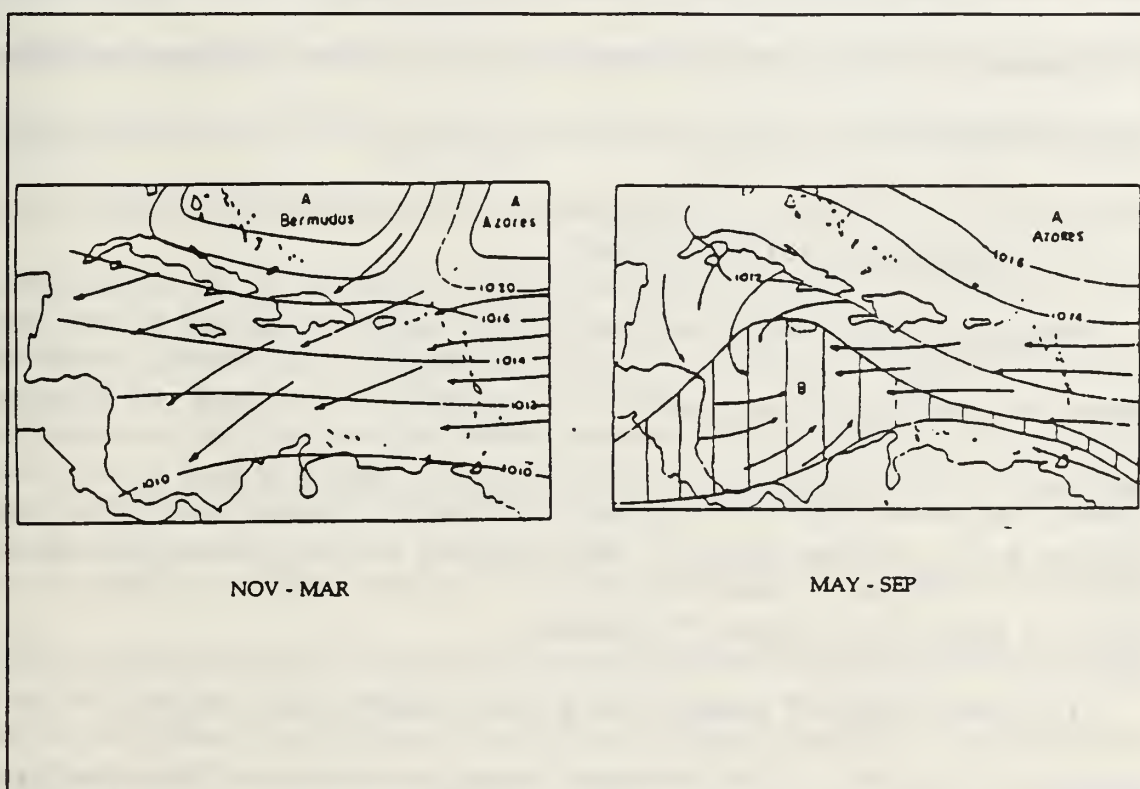


Figure 4 Wind regime in the Caribbean
(from Pujos et al., 1986)

In the windy season the character of the ITCZ is different. At the longitude of the Caribbean, the ITCZ remains in the Southern Hemisphere and influences the Caribbean region by producing a confluence in the streamline field, leading

to steady and strong northern trade winds (easterlies) over the whole basin (Fig. 4 Nov-Mar, Pujos et al.1986). A transition stage is mainly characterized in the Western Caribbean by the slow change in the wind direction and lower wind speed over the entire basin.

The variation in latitude of the ITCZ through the year allows the easterly wind to exert more or less influence in the region. As the ITCZ appears or departs the basin, the fetch of the easterlies changes with a subsequent change in the wind stress. During the humid season there are low winds and extensive development of strong vertical convection with severe thunderstorms in the Western Caribbean.

C. THEORETICAL BACKGROUND

Satellite altimetry began with the GOES 3 satellite, launched in 1975, and proved that satellite altimetry could be accomplished from space. An altimeter was placed on board SEASAT in 1978. However, only 100 days of data was collected due to a system failure. In 1985, GEOSAT was put in the space with an improved version of the SEASAT altimeter.

The Navy GEOSAT mission has proven satellite radar altimetry to be a versatile and powerful tool for the remote sensing of the oceans. These data have been used to support Navy operational requirements in many meteorological and oceanographical areas. Collateral products such as wind speed and significant wave height (SWH) have been obtained with good accuracy for many remote

regions of the world.

The GEOSAT primary mission was to improve knowledge of the marine gravity field. After successfully accomplishing this goal, it was maneuvered to alter its orbit to one very close to the original of SEASAT orbit, with a period of 17 days. This stage of the mission is known as the GEOSAT Exact Repeat Mission (ERM).

The altimeter used a 13.5 GHz nadir-looking, pulse compression radar whose major characteristics are listed in Table 1. A pulse-limited mode of operation was used in which the intersection of the pulse with the ocean surface defines a region with small lateral extent compared to that defined by the antenna beam width. The earliest signal return comes from the wave crests, then reflecting facets deeper in the waves contribute, accompanied by an increase in the illuminated area within a range resolution cell, until a point is reached where the back edge of the pulse envelope reaches the wave trough. Beyond this point, the signal amplitude remains constant theoretically. In fact, the antenna gain pattern is not constant and thus imparts an exponential decay in amplitude. Together with a very precise clock, the resulting wave form and the sharp leading edge of the return wave form the basis for a precise height estimation. The half-power point conforms closely to mean sea level. The satellite tracks the location of every point and these heights are telemetered to the ground.

Other geophysical measurements such as significant wave height (SWH) are

TABLE 1. GEOSAT CHARACTERISTICS

Center frequency	13.5 Ghz.
Repetition period	17.05 days
Resolution	10 km/pix
Swath width	1.8 - 8.1 km.
Pulse width	102.4 ms
Band width	.3 Ghz.
Antenna beamwidth	2.0 degrees

possible from the shape of the wave crest. In addition, the altimeter uses an Automatic Gain Control (AGC) loop to normalize the amplitude of the return signal from the ocean surface. Properly calibrated, the return signal is related to the wind speed. The greater the wind speed, the lower the cross section thus the weaker the return signal from the sea surface.

The effect of the environment on the outgoing and returned pulse are very significant and must be corrected. The ionosphere free electron content varies from day to night (very few electrons at night), from summer to winter (fewer in

summer) and as a function of the solar cycle (fewer during solar minimum). Depending on the time of observation, the number of electrons in the ionosphere can induce an error from 0.2 to 20 cm in a 13.5 Ghz radar. In the troposphere the mass of air and water vapor content affects (slows down) the speed of light (GEOSAT pulse). The mass of dry air induces an error of 230 cm and is reasonably constant, however, the water vapor induced error varies from 6 to 30 cm at the GEOSAT frequency. In the Caribbean Sea, the atmospheric water vapor content is often high, with high variability, especially in the ITCZ. Water vapor content is corrected by using the FNOC water vapor model or removed during the tilt and bias removal. However, the water vapor distribution in the ITCZ may not be sufficiently well resolved. This will result in errors that will blur the small oceanic features that are the object of this study. Because there is only one channel on the altimeter, corrections for ionospheric and tropospheric effects are made by using Fleet Numerical Weather Center (FNOC) numerical models.

Unfortunately, data flow from GEOSAT diminished over time, apparently due to the increase of sun spot activity that caused the exosphere to expand as documented in Lilly (1988). This results in increased density at 833 km (orbit height) and thus increased the drag on the satellite. GEOSAT was very sensitive to drag as it must operate in a nadir looking mode. If the satellite is forced off nadir, data is lost. This apparently happened in 1987-1988 resulting in fewer data points retrieved over several months, interrupting the time series of data used in this work. The GEOSAT ceased operations in 1990.

Several wind speed algorithms were analyzed in Dobson et al. (1987). They were: Brown's, Chelton and McCabe's, Goldhirsh and Dobson's, Chelton and Wentz's and the smoothed Brown's algorithms. Each algorithm was compared with buoy data. Dobson et al. concluded that the Brown's and smoothed Brown's algorithms were the most accurate. Wind speed data using the smooth Brown's algorithm will be used in this study.

Theoretically, the satellite measured the SWH within .5 m or 10 percent, and estimated the wind speed between 1 and 18 m/s with an error of ± 1.8 m/s. Comparisons with ground truth data have been made to validate the GEOSAT data, e.g. Shuhy et.al.(1987), Dobson et.al. (1987) and Tournadre and Ezraty (1990). This last study concluded that the altimeter underestimates the SWH by 20 cm with an uncertainty of 42 cm and the wind speed by 0.3 m/s with an uncertainty of 2.0 m/s. These results were in good agreement with the results of the previous validation studies.

III. METHODOLOGY

The data set used in this thesis is the GEOSAT ERM data edited by Zlotnicky et al. (1989) collected during 1987-88 over the Caribbean Sea. These data were obtained from the NASA Ocean Data System (NODS) at the Jet Propulsion Laboratory (JPL).

The raw data were corrected for ocean and solid earth tides, atmospheric pressure loading (the so-called inverse barometer effect), range delays for wet and dry tropospheric content using FNOC formulae as described in Cheney et.al (1987), and ionospheric range delays. The corrected heights were then edited by deleting data outside the range -14000 to 1000 cm, removing spikes from data using a series of quadratic fits and interpolated to a fixed geographical grid with a 7 km spacing along the ground tracks (Zlotnicky et al., 1989).

The automatic tracking algorithm for the altimeter height measurement fails over land. In a restricted area of study, such as the Caribbean Sea with many islands and nearby continental land masses, much of the height data is flagged. All flagged data was eliminated, in order to diminish the probability of data error.

A. HEIGHT CORRECTIONS

The gridded height data were objectively analyzed. Anomalous data, isolated points and shorts arcs segments were discarded. An example of the raw

data is shown in Fig. 5. The next step was to remove the marine geoid contribution to the sea surface height in the altimeter signal. Unfortunately, the

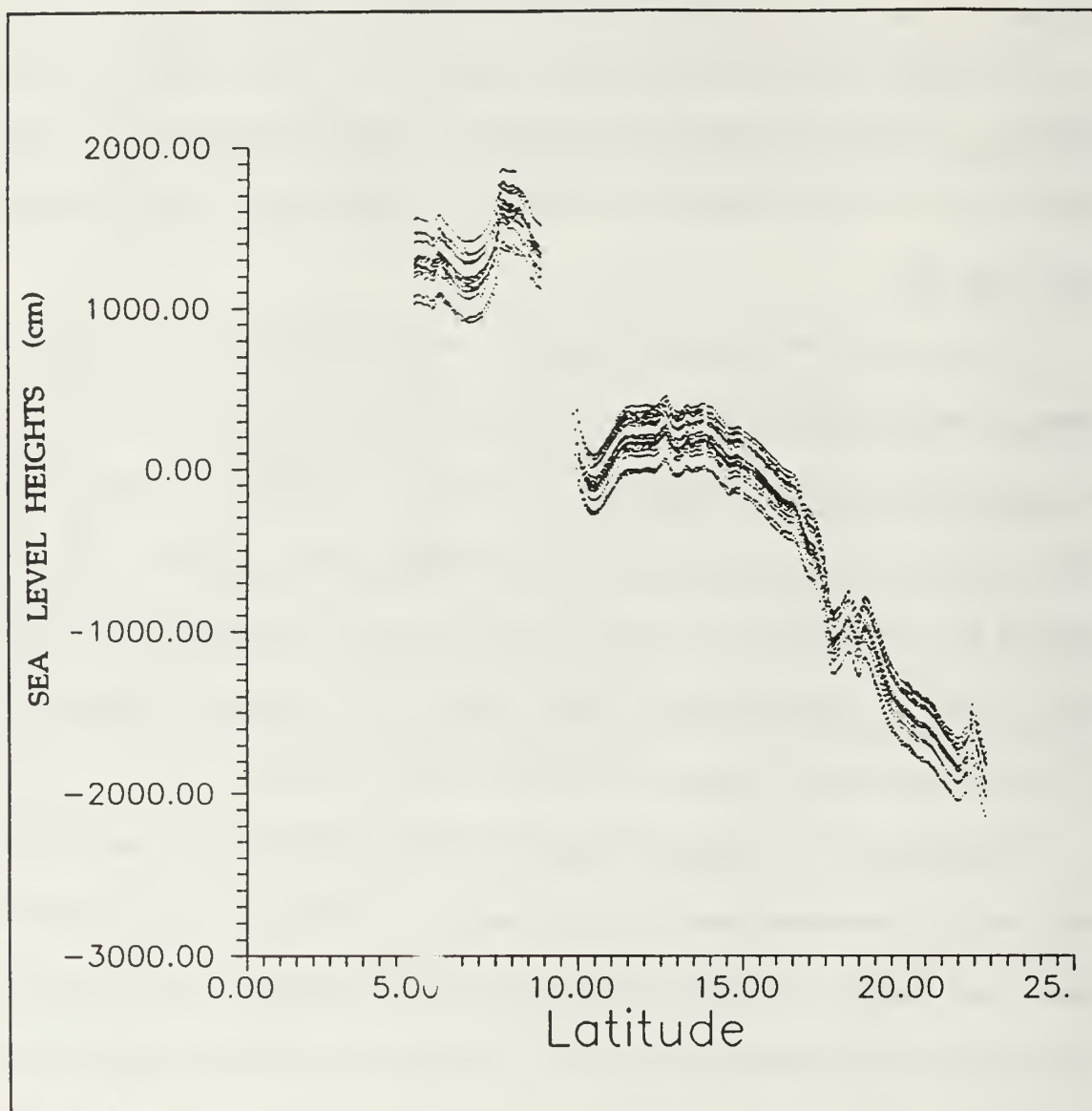


Figure 5 Raw data from orbit 2843 A (an ascending orbit with equatorial crossing at 284.3°E or 75.7°W).

technique for the removal of the mean marine geoid also eliminates the time invariant component of geostrophic oceans currents. In this case the mean Caribbean current is removed. This will be a limitation of altimetry until an

independent marine geoid is available and can be removed from the altimeter data independently.

As is explained in Chelton et al. (1990), because of data dropouts, the number of repeat samples of sea surface elevations differs at each along-track grid points. With the large random orbit errors (about 3 m standard deviation) characteristic of the GEOSAT data, the statistical reliability of a simple arithmetic mean sea level at a specific grid location, x , can be very sensitive to the number of repeat samples, $N(x)$. As $N(x)$ varies along the track, orbit error contamination results in artificial jumps in the mean sea level profile.

In this thesis, a method suggested by Chelton et al. (1990) was implemented. This method gives a more reliable estimate of the mean sea level, without the irregular along-track jumps inherent to the arithmetic mean procedure. If the orbit error consisted of a simple bias, then the orbit error contamination of mean sea level could be eliminated by first computing the arithmetic mean of along-track differences,

$$\overline{\delta h}(x_m) = \left(\frac{1}{N_m} \right) \sum_{n=1}^{N_m} h_n(x_{m+1}) - h_n(x_m)$$

where h is the altimeter height measurement, the indices n and m refer to the cycle number and the position along the track, respectively, and N_m is the number of cycles for which height measurements at X_m and X_{m+1} both exist. The

mean sea level can then be obtained by summing (integrating) the mean differences along the ground track,

$$\bar{h}(x_M) = \bar{h}_o + \sum_{m=1}^M \delta \bar{h}(x_m)$$

The method of estimating the initial value, h_o (equivalent to establishing a constant of integration), is estimated by the arithmetic mean for the grid point x_{\max} , at which maximum data points for each arc segment occurred,

$$\bar{h}_o = \bar{h}(x_{\max}) - \sum_{h(x_o)}^{h(x_{\max})} \delta \bar{h}(x_m)$$

The calculated mean sea level, shown in Fig. 6, is then removed from each orbit of the raw heights along each ground track (Fig. 7).

In the residual sea level heights (Fig. 7), most of the errors are those due to orbit uncertainty. However, occasionally there is an error as the satellite reaches an island or continent (the footprint signal is contaminated by the nearby land giving a big spike in the record), which must be removed before further processing of the data. Fortunately most of the satellite orbit errors have very long wavelengths, which can be seen as tilt (inclination of one pass to another) and bias (offset of one pass to another) in the data along an orbital track. Therefore this error is removed by applying a linear least-square fit to each of the orbit segments along the orbit track (Fig. 8). Of course, this tilt and bias removal technique will also remove any linear trend in the dynamic height topography (Maul et al., 1988). It also attenuates information about temporal sea level

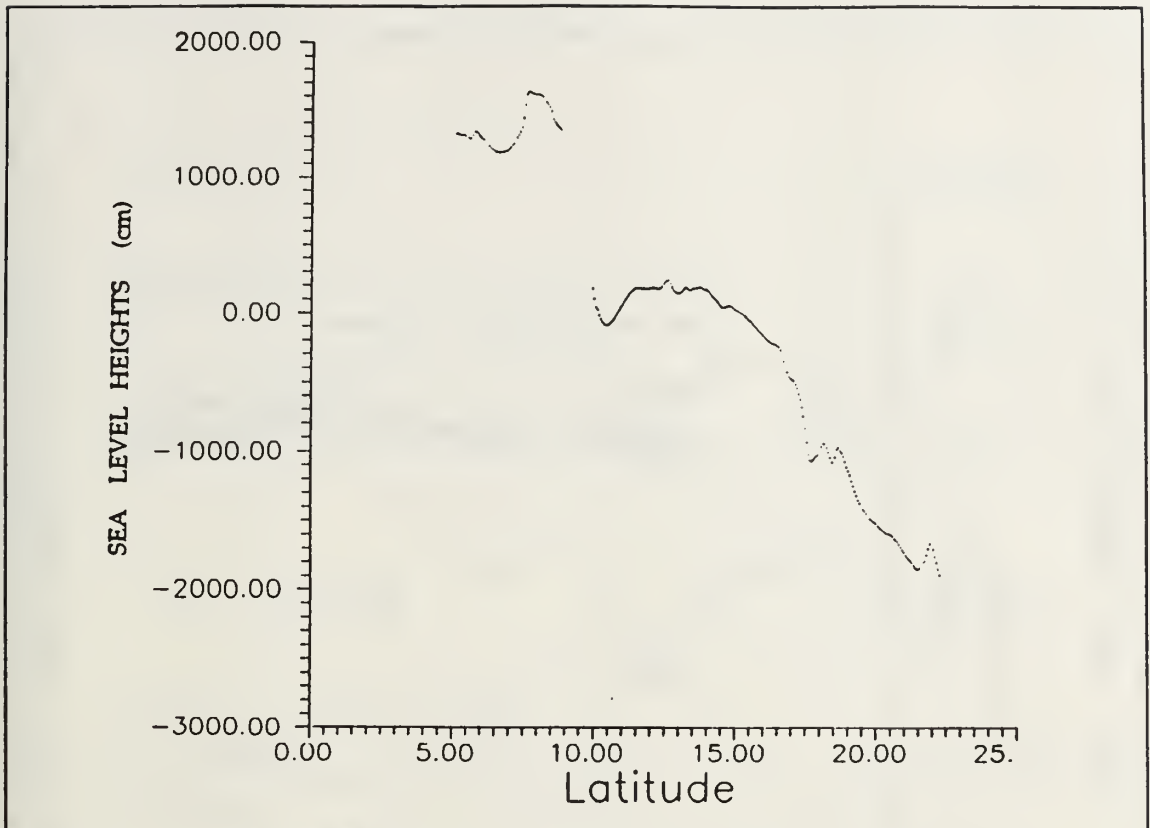


Figure 6 Mean sea level for GEOSAT Orbit 2843 A

differences with half-width equal to or greater than the length of orbit segment from which the tilt and bias are calculated (Hansen and Maul, 1990). The residual sea level signal is suitable for observing sea level variations associated with temporal varying quasi-geostrophic mesoscale surface features. Finally, the data shown in Fig. 9 were smoothed using a running mean average using five consecutive points to remove the small scale noise.

As previously mentioned, the mean sea level computed in this manner includes the time invariant geostrophic circulation signal which is removed along with the geoidal component. Therefore, the only features that can be detected by this method are the ocean features with temporal sea level variability.

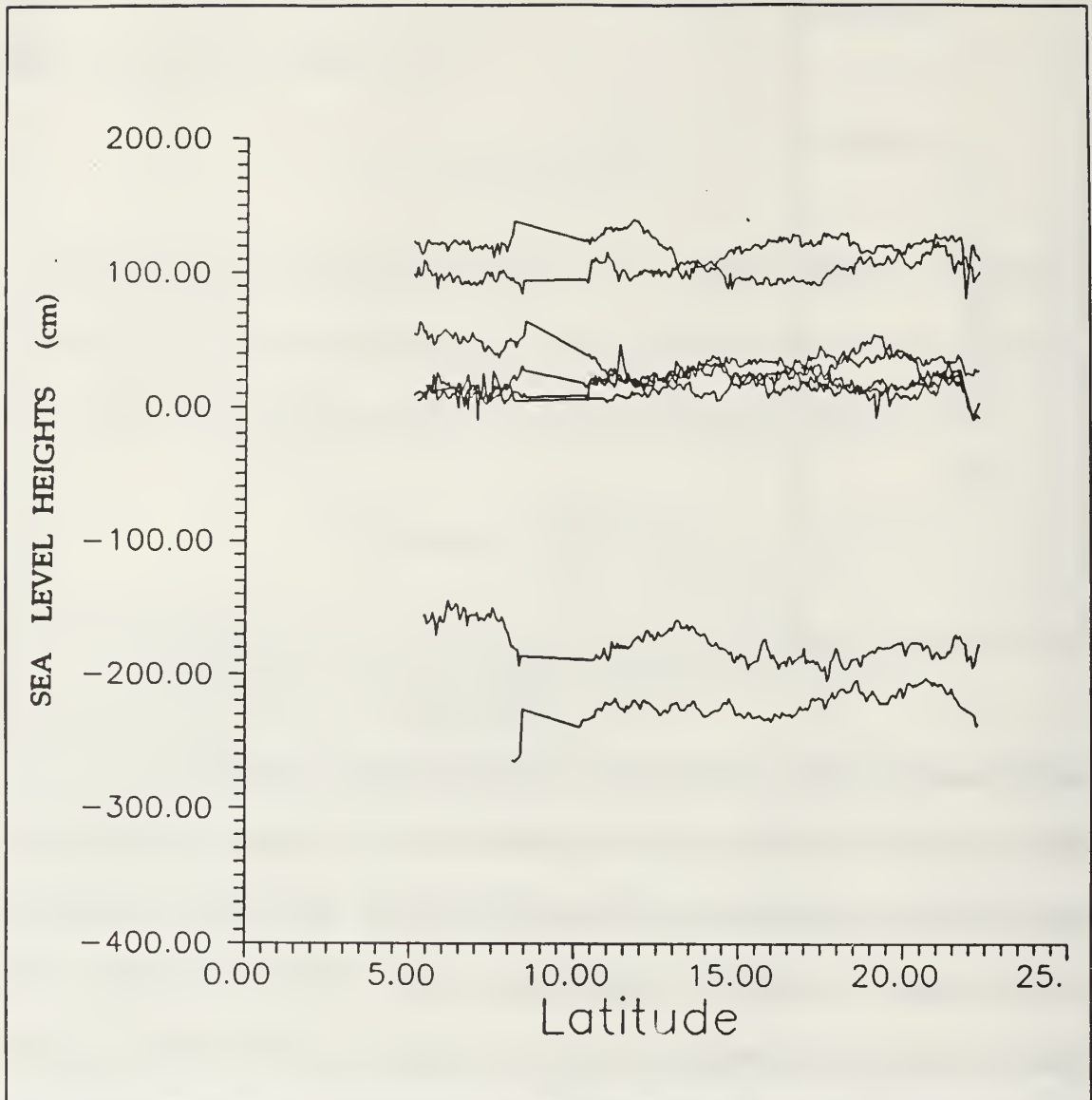


Figure 7 Heights after demeaning process GEOSAT Orbit 2843A

In an attempt to observe the horizontal spatial structure, contours of the height fields were computed. The nature of the GEOSAT orbit is such that two ascending tracks are separated by 1.48 of longitude and by 3 days in time. As time progresses, tracks are filled in an eastward direction. Fig. 10 shows the GEOSAT coverage over the Caribbean Sea. Orbit track 2791 D, marked A will be

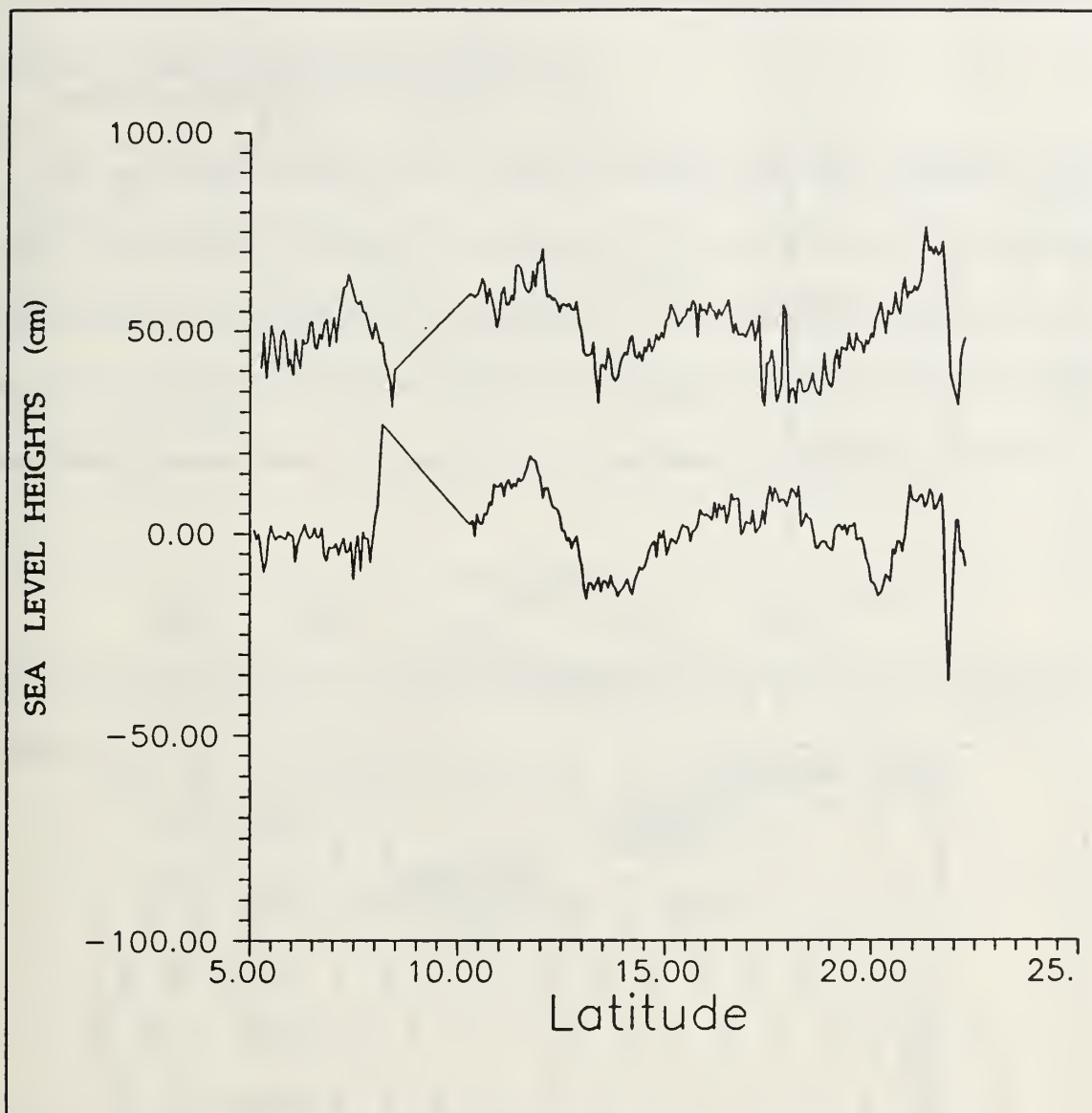


Figure 8 Heights after orbital removal (shifted 50 cm).

variability at each position along each of the track sub-orbits is calculated and used for collinear track analysis and orbit track 2732 D, marked B will be used for contouring height anomaly time series in the discussion chapter. Maps of sea surface heights anomalies for each 17 day period were calculated over the Caribbean in a quasi synoptic sense.

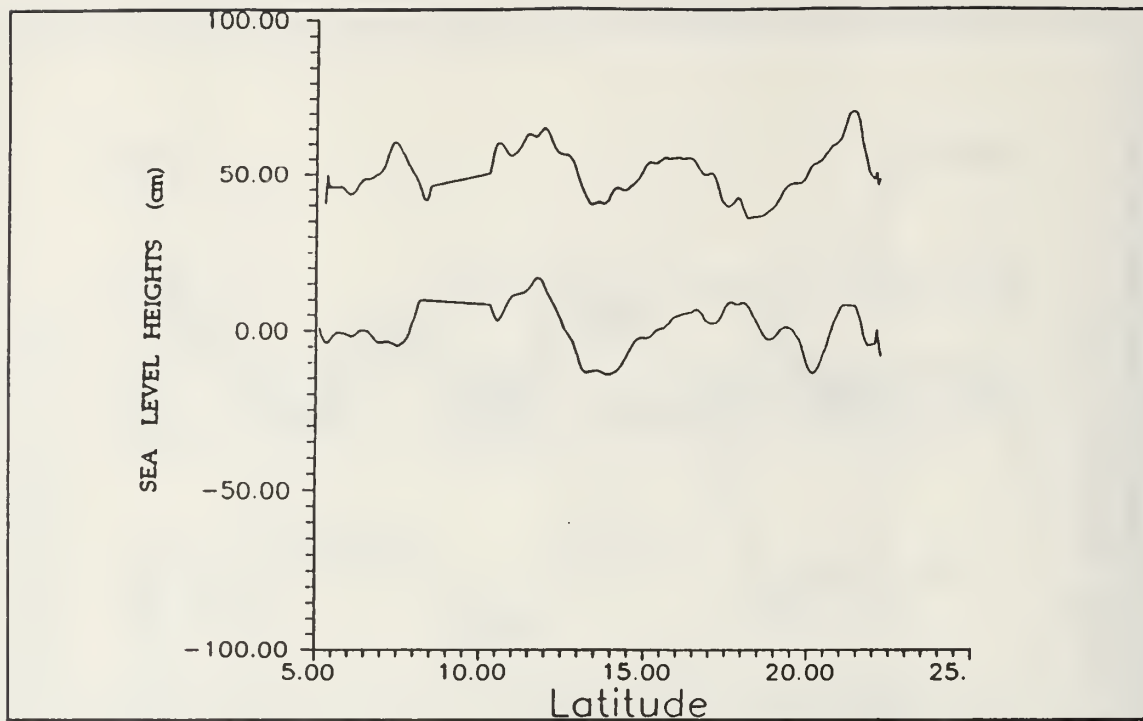


Figure 9 Heights after smoothing process GEOSAT orbit 2843A

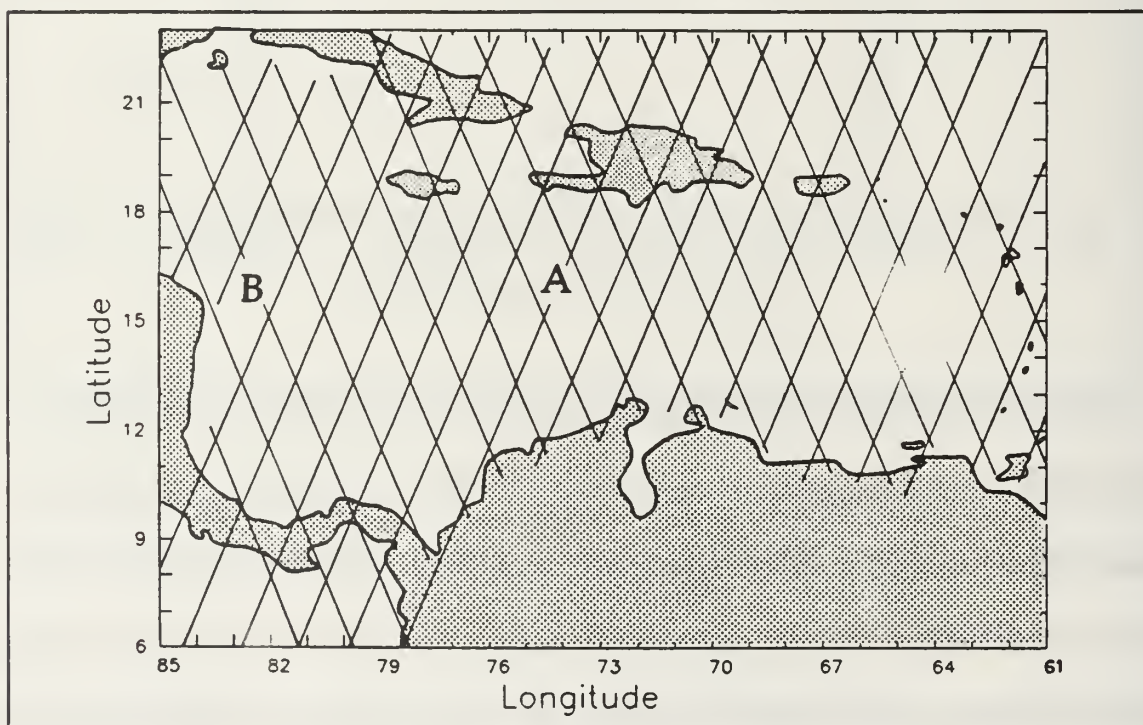


Figure 10 GEOSAT orbit tracks over the Caribbean Sea

Finally, the root mean square variability at each position along each of the track sub-orbits is calculated and discussed.

B. WIND SPEED CALCULATION

As previously noted in the theoretical background, the Automatic Gain Control AGC is used to derive the wind speed at the sea surface by using the backscattering cross section of the return pulse. This quantity is known as σ_0 . In this study, the smoothed Brown's algorithm was used to compute the wind speed from the altimeter radar cross section σ as described in Dobson et.al. (1987),

$$W = \sum_{n=0}^5 a_n \sigma_0^n$$

$$\sigma_0 < 15 \text{ decibels,}$$

where

$$a_0 = -15.383$$

$$a_1 = 16.077$$

$$a_2 = -2.305$$

$$a_3 = 0.09896$$

$$a_4 = 0.00018$$

$$a_5 = -0.00006414$$

The condition $\sigma_0 < 15$ decibels implies that the algorithm is restricted to wind-speed values greater than 2 m/s. All data flagged for $AGC > 50$ db and $AGC < 16$ db as well as data with the satellite attitude greater than 1° were dropped from the analysis.

The nature of the GEOSAT orbital coverage over a region does not permit the use of the wind speed data in a synoptic form. An alternative is to use the data to describe climatic features with an oscillation larger than two times the frequency of the sampling, i.e. 34 days. Extensive averaging of the wind data has to be made to have representative values that "smooth" the higher frequency phenomena that is aliased by the 17 day sampling of GEOSAT.

To achieve this goal, the wind data from each 17 day ERM period was averaged within a grid of one degree of latitude by one degree of longitude throughout the whole Caribbean Basin. After calculating a value per grid point, three consecutive 17 day periods were averaged to give a representative wind field per ERM period. Consecutive periods were averaged to generate a seasonal mean average of the wind speed. The following equation summarizes the technique,

$$\overline{W}_m = \frac{1}{P} \sum_{i=1}^P \frac{1}{N_m} \sum_{j=1}^{N_m} w_m$$

where W_m is the monthly mean wind speed at the center of every one degree square in the grid, w_m is every wind speed sample point along the track, N_m is number of points per square in the grid and P is the number of ERM periods averaged. Time series of selected points in the basin were obtained which show the characteristic climatic wind field for each season, as will be discussed later.

IV. RESULTS

A. HEIGHT ANOMALY ANALYSIS

When examining the height field one must remember that this variability must be superimposed on the mean sea level. The mean sea level was removed by the geoid and tilt and bias correction. Wust (1963) and Gordon (1967) have shown that the north Caribbean Sea is dynamically higher than the southern part by an average of 20 dynamic centimeters with upwelling near the South-American coast and convergence in the north.

Thus, the positive and negative values are shown here with respect to the zero level and not with respect to the real mean sea level. Fig. 11 illustrates this point. This is especially important for the interpretation of the direction of the mesoscale features present in the basin. In other words, negatives

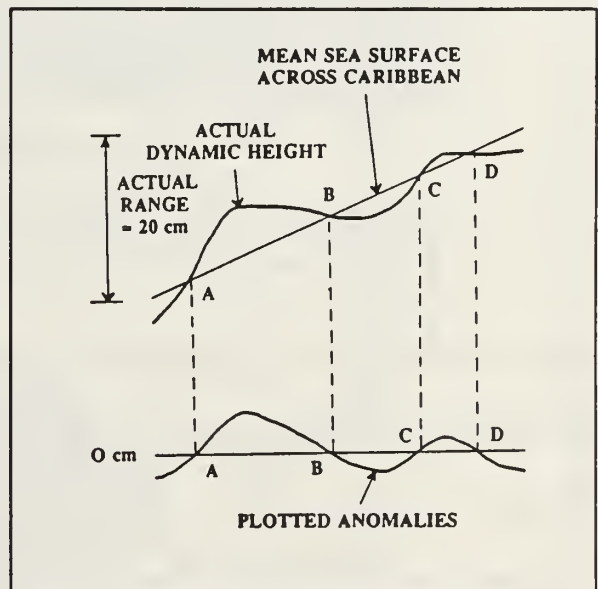


Figure 11 GEOSAT detection

values should be interpreted as "less positive", unless the strength of the negative height signal is strong enough (≈ -20 cm) to result in a negative slope in true

dynamic sea level. The attempt here is to observe significant anomalies, their magnitude, and to track them as they travel through the basin.

If insufficient data were available over the Caribbean during a given ERM period, the contour fields lined up along orbit tracks. When this was detected the contour field chart for the period was discarded. Note that data along individual tracks during such a period might be available but the contour field (of all tracks) was discarded. Only three sets of ERM contour sequences were long enough to follow mesoscale features over time. The date for each ERM period is the middle day of each 17 day ERM period; the contour interval is 10 cm.

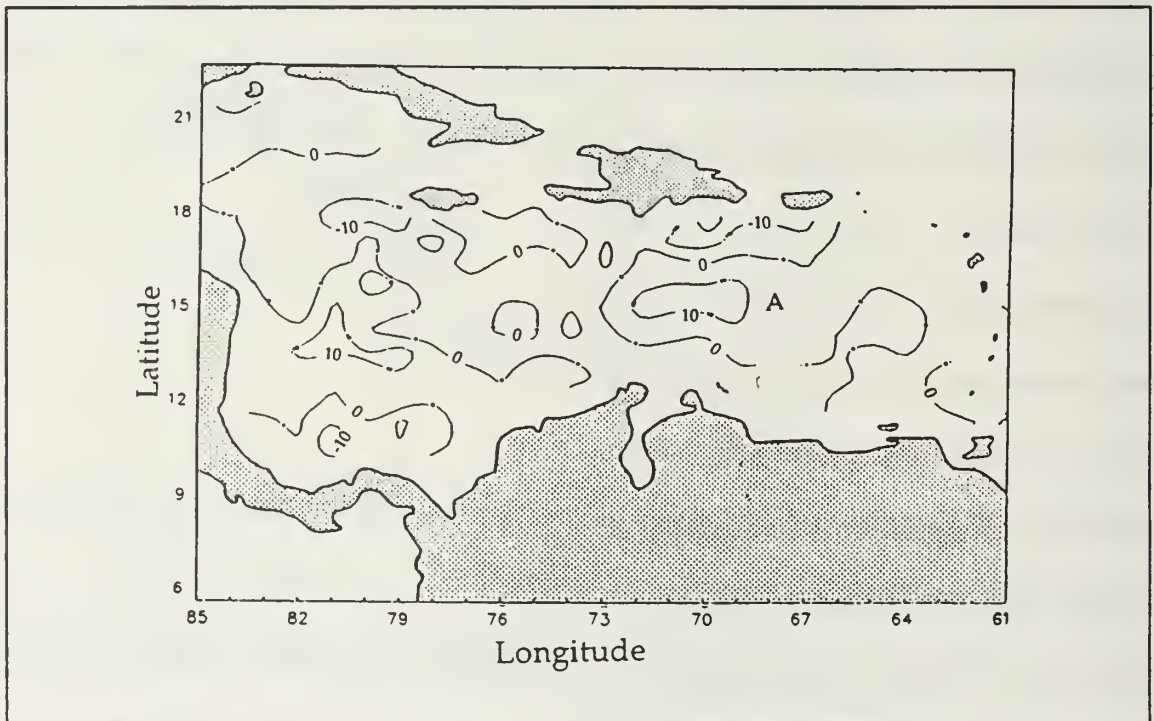


Figure 12 Mesoscale variability 14 May 1987
contour interval is 10 cm.

The first sequence is from May 14 to July 21 of 1987 (Figs 12 to 16). On May 14, positive anomaly, marked A, is observed. On May 31 feature A has moved

about 30 km to the southwest. On June 17, feature A has doubled its strength to +20 cm and is displaced 360 km to the west, indicating an approximate speed of 24 cm/s. At this time a negative (cyclonic) signal feature, marked B, appears in

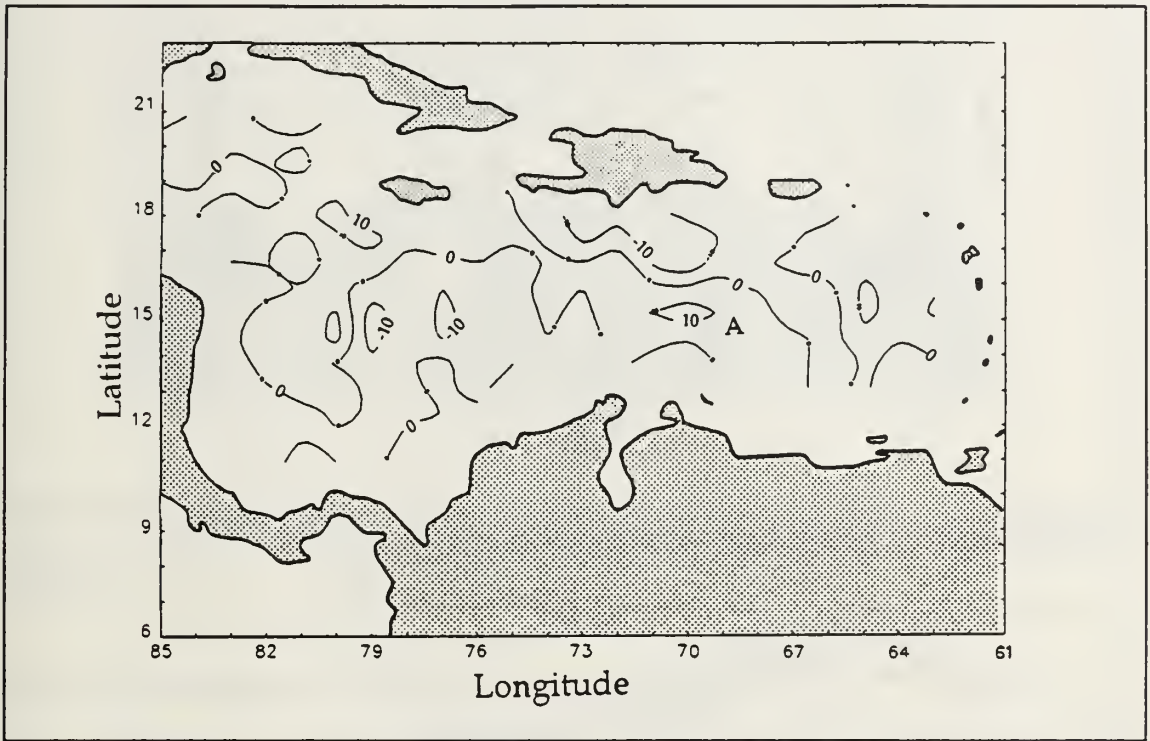


Figure 13 Mesoscale variability 31 May 1987
contour interval is 10 cm.

the southwest part of the basin. In the next period, July 4, feature A has continued to moved to the west about 230 km, at 15 cm/s, with a diameter of 290 km and its height anomaly is now more than + 30 cm. Feature A has the character of an anticyclonic eddy moving along with the Caribbean Current. On July 21, the eddy marked A has moved 170 km further to the west, with an apparent speed of 12 cm/s; its relative size is about the same but its dynamic anomaly signal has diminished by 10 cm. Feature B has reappeared in the same

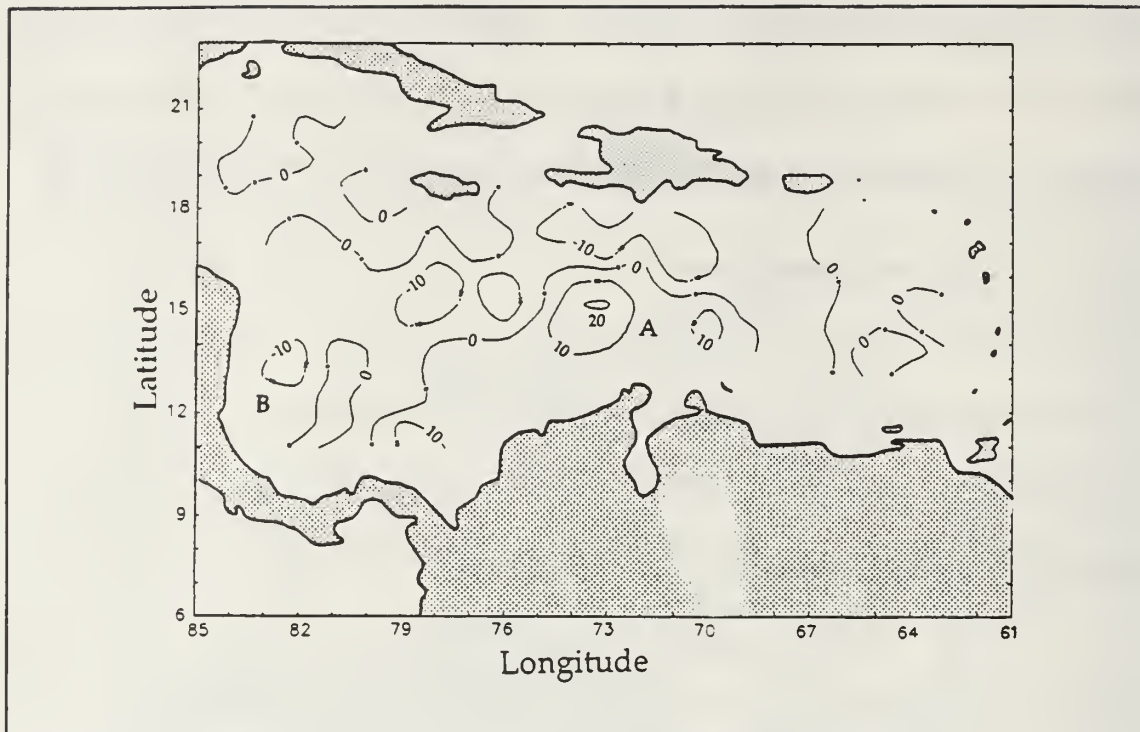


Figure 14 Mesoscale variability 17 June 1987

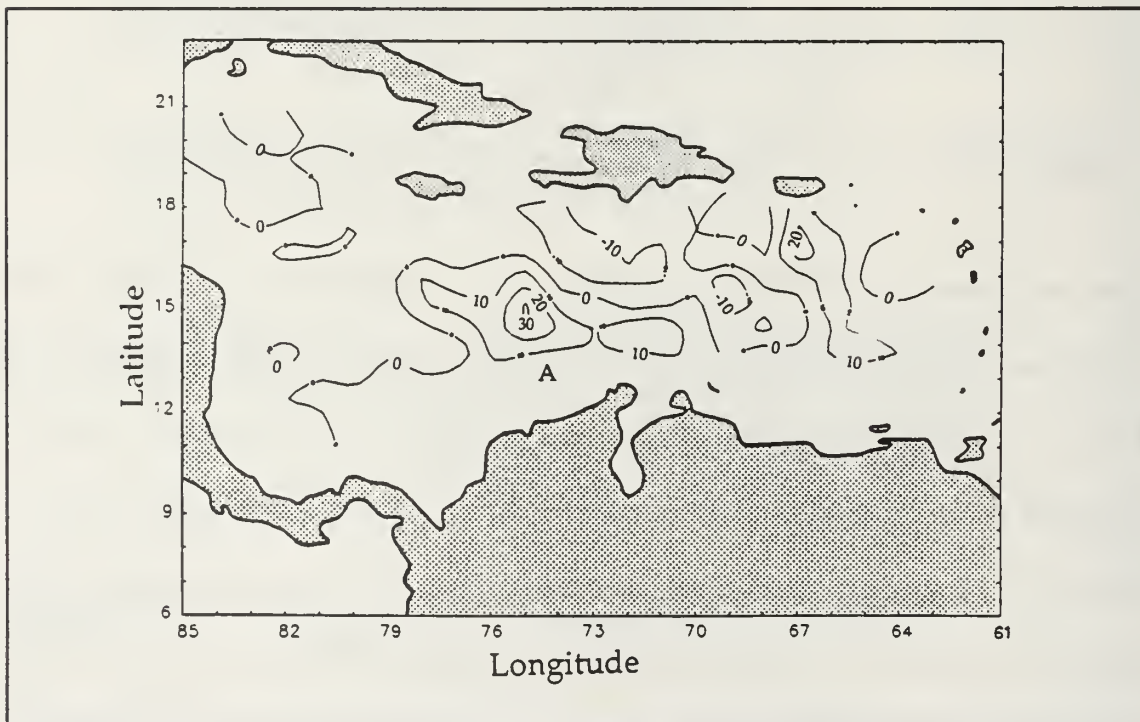


Figure 15 Mesoscale variability 4 July 1987

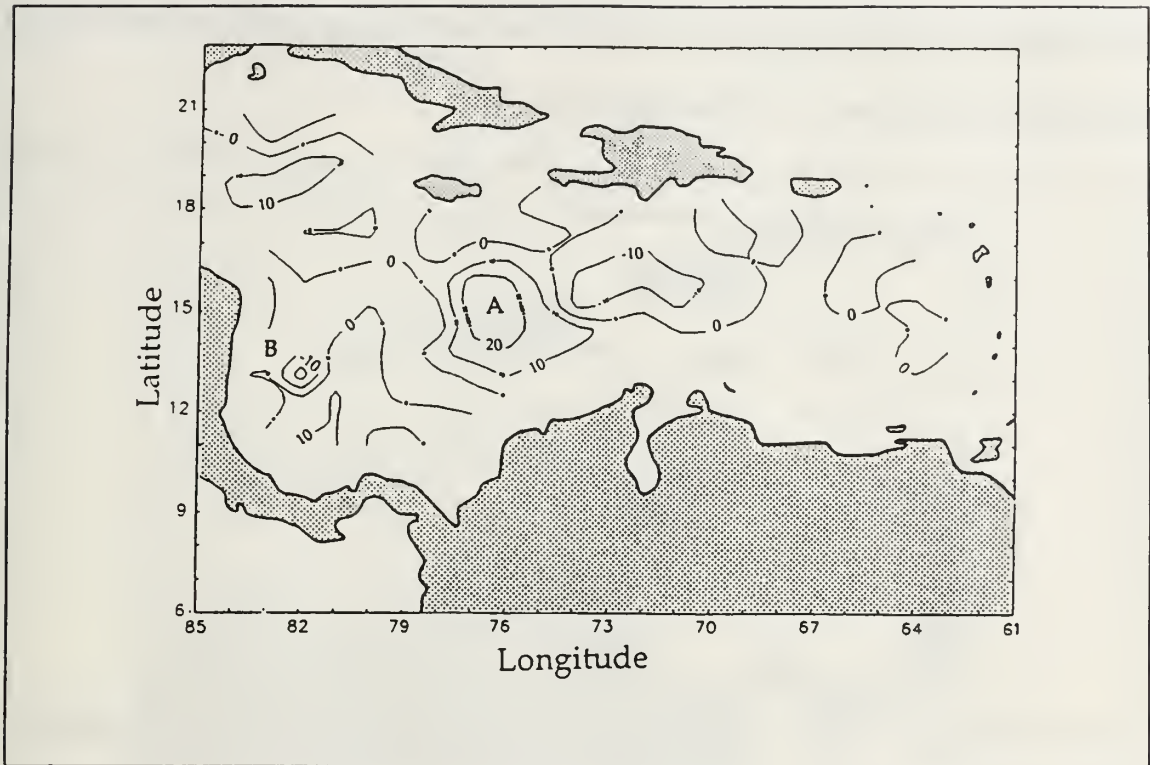


Figure 16 Mesoscale variability 21 July 1987
contour interval is 10 cm.

position and its signal is of less than -20 cm. This appears to be a small stationary cyclonic eddy formed independently from the main flow of the Caribbean current. This cyclonic anomaly matches in position and strength the one that appeared in the models in Gordon (pers. commun.,1990) and Thompson (pers. commun.,1990).

Unfortunately, observations were interrupted at this point because of absence of enough data to generate contour charts.

The next observations were of three periods in April and May 1988, Figs 17, 18 and 19. On April 13 the main feature present is a positive anomaly in the center of the basin, marked D. On April 30, feature D has doubled its height to

more than 20 cm and has moved 120 km from its previous position, indicating a translation rate of 8 cm/s, to the northwest.

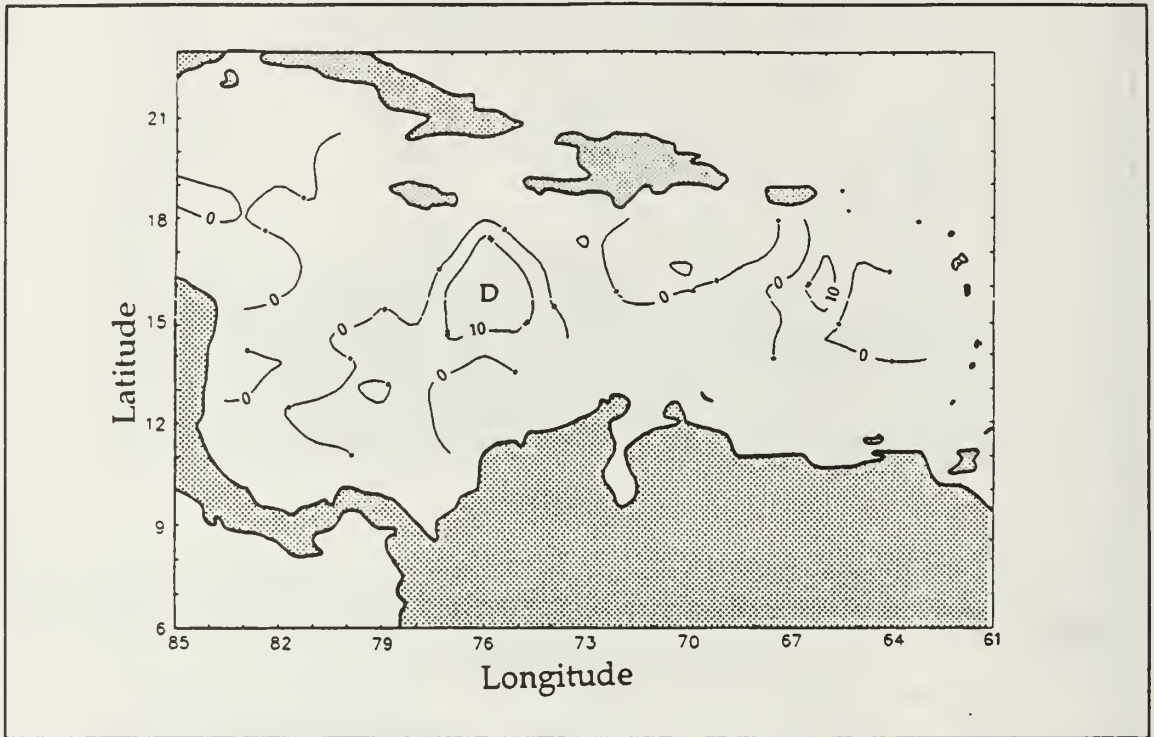


Figure 17 Mesoscale variability 13 April 1988
contour interval is 10 cm.

By May 17, feature D has the same +20 cm signal and has been displaced 180 km to the west (11 cm/s). Feature B is again present in the same position as it was observed in 1987.

The last continuous series that could be obtained by this method was in September - November 1988, Figs 20 to 22. On September 30, 0 cm contour can be followed along the full length of the Caribbean. These contours suggest that the Caribbean Current makes a pronounced meander in the Venezuelan Basin. On Nov 3, the two contours (0 cm) can also be followed along the full length of

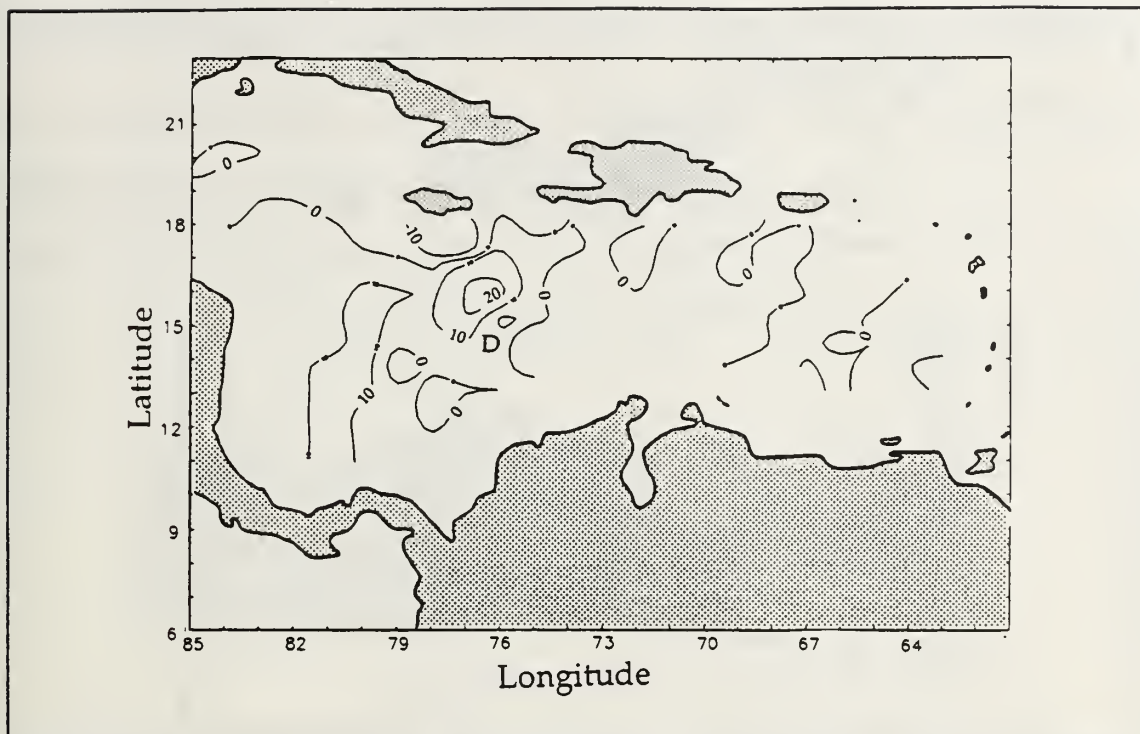


Figure 18 Mesoscale variability 30 April 1988

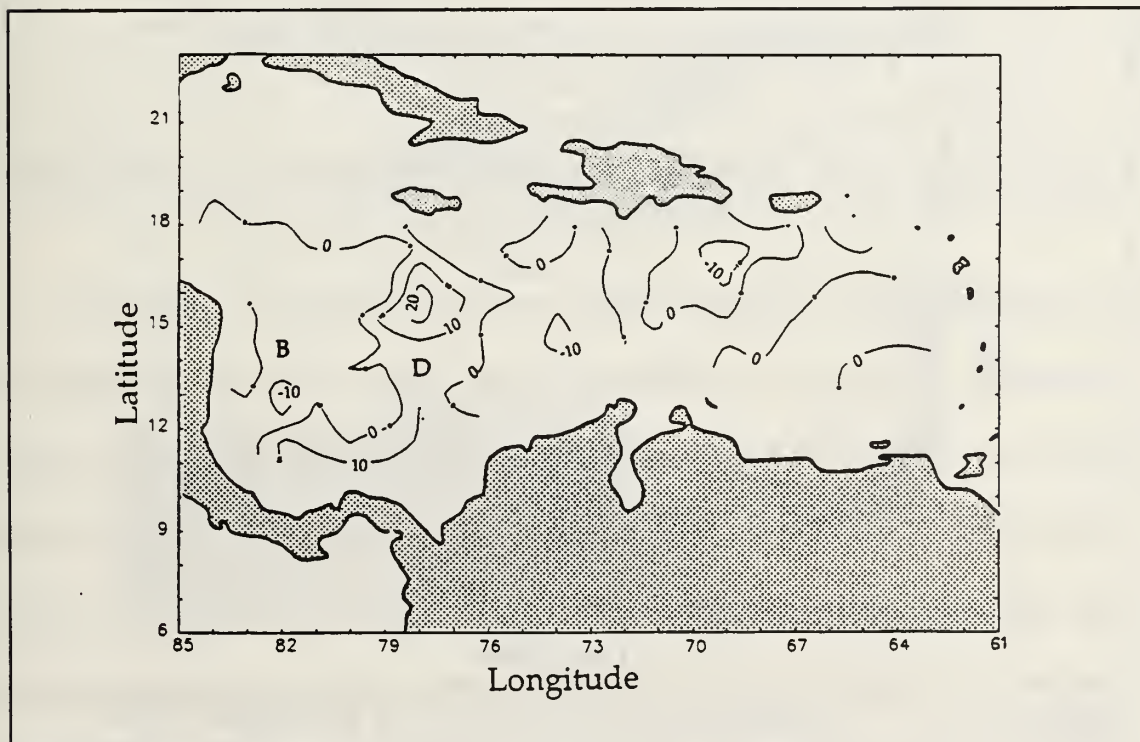


Figure 19 Mesoscale variability 17 May 1988

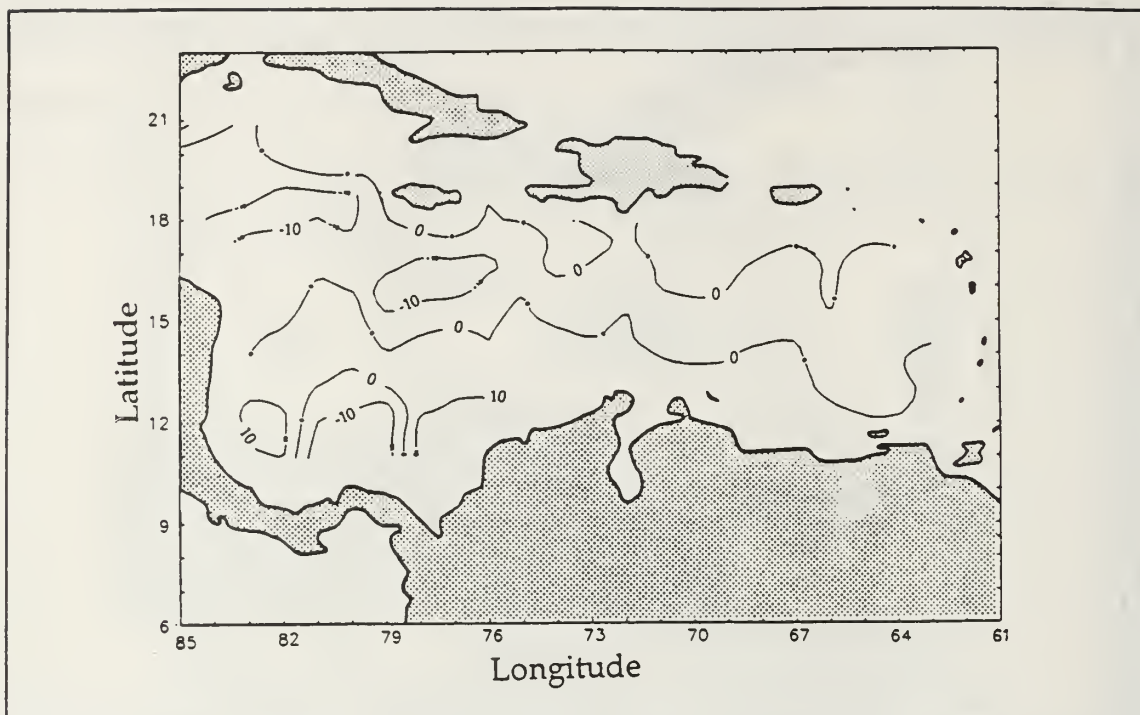


Figure 20 Mesoscale variability 30 September 1988

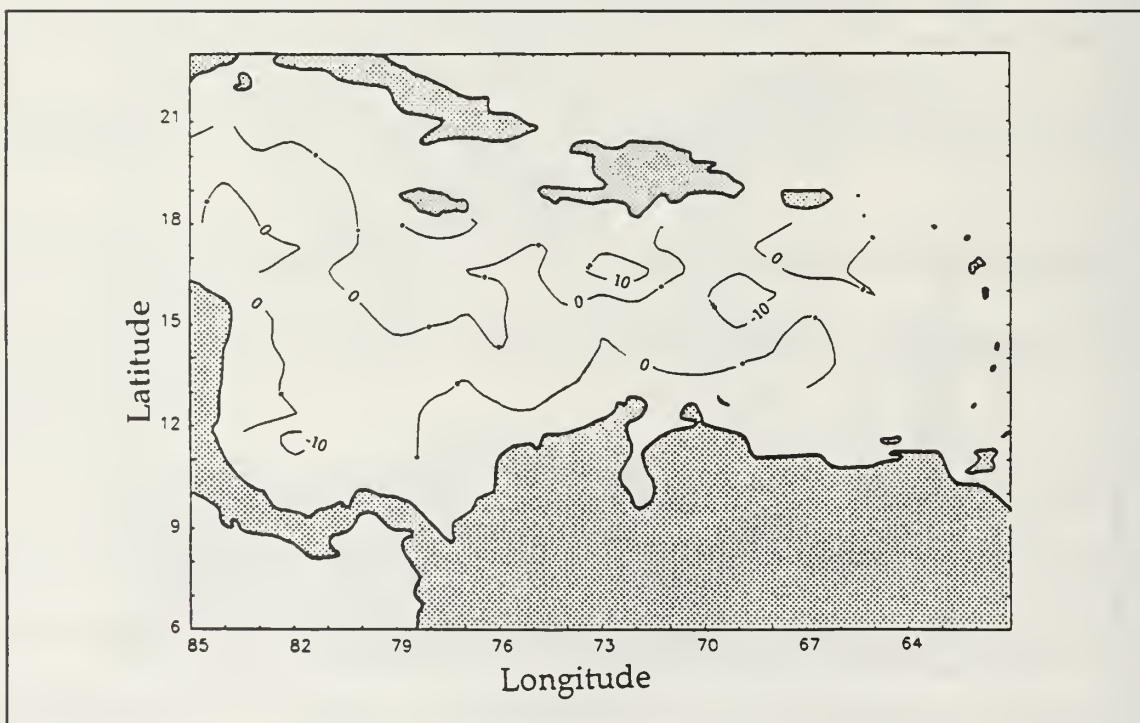


Figure 21 Mesoscale variability 3 November 1988

the basin. The northern one shows the Caribbean Current meandering along the basin. No mesoscale eddies were tracked during this time period in the Caribbean Current; feature B was again present in the same area.

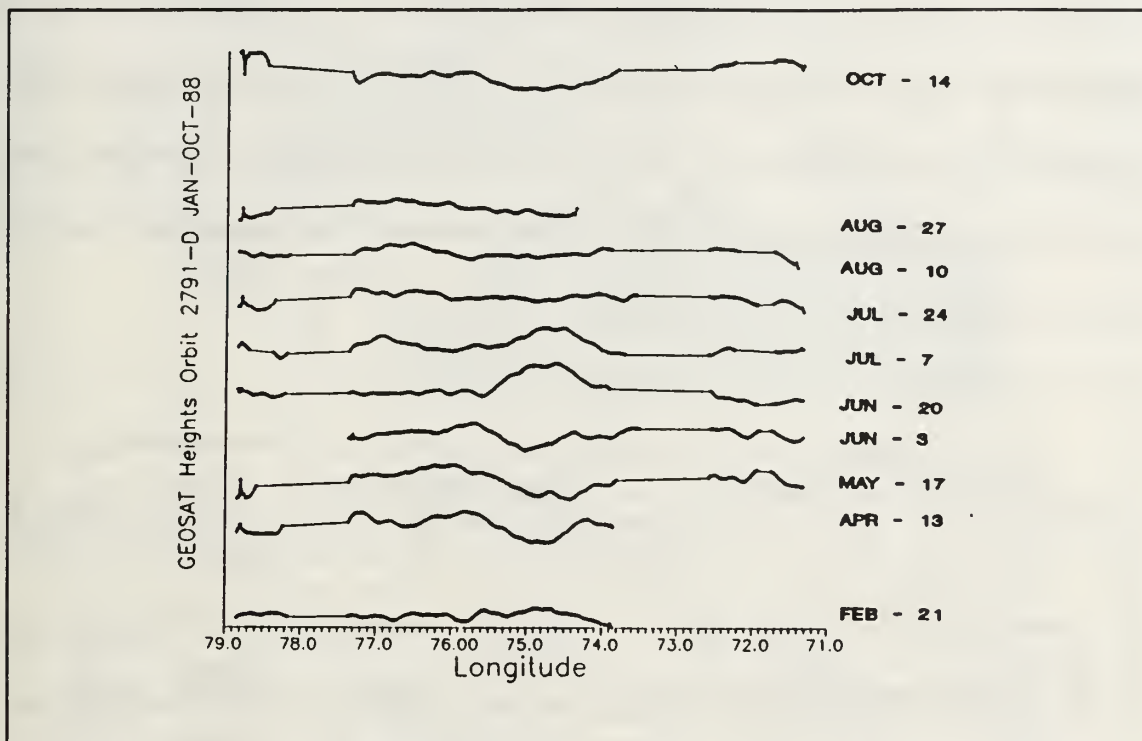


Figure 22 Collinear tracks Orbit 2791 D (a descending orbit with equatorial crossing at $279.1^{\circ}\text{E} = 80.9^{\circ}\text{W}$)

An analysis of collinear tracks was made with orbit A from Fig. 6 over the two years (Fig. 22). This analysis showed two distinctive modes in the behavior of height anomalies. The height variations were higher from April to June than during the rest of the year in the northern half of the Basin ($74^{\circ}\text{W} - 76^{\circ}\text{W}, 13^{\circ}\text{N} - 18^{\circ}\text{N}$). This behavior is closely related to the seasonal variation of the trade winds during the year and is inversely proportional to the trade wind intensity. During the stronger wind season, the Caribbean Current is apparently more

stable. When the wind relaxes, the current is apparently less stable and mesoscale features appear.

In order to examine the behavior of the cyclonic feature in the Southwestern Caribbean, a time series of heights for Orbit B, in Fig. 6, was examined. Fig. 23 suggests that this is a quasi-permanent feature which appeared at various times throughout the year under this particular track. Of course it is detected only because it move; (the geoid removal technique removes truly permanent features) and only when it is under this particular track.

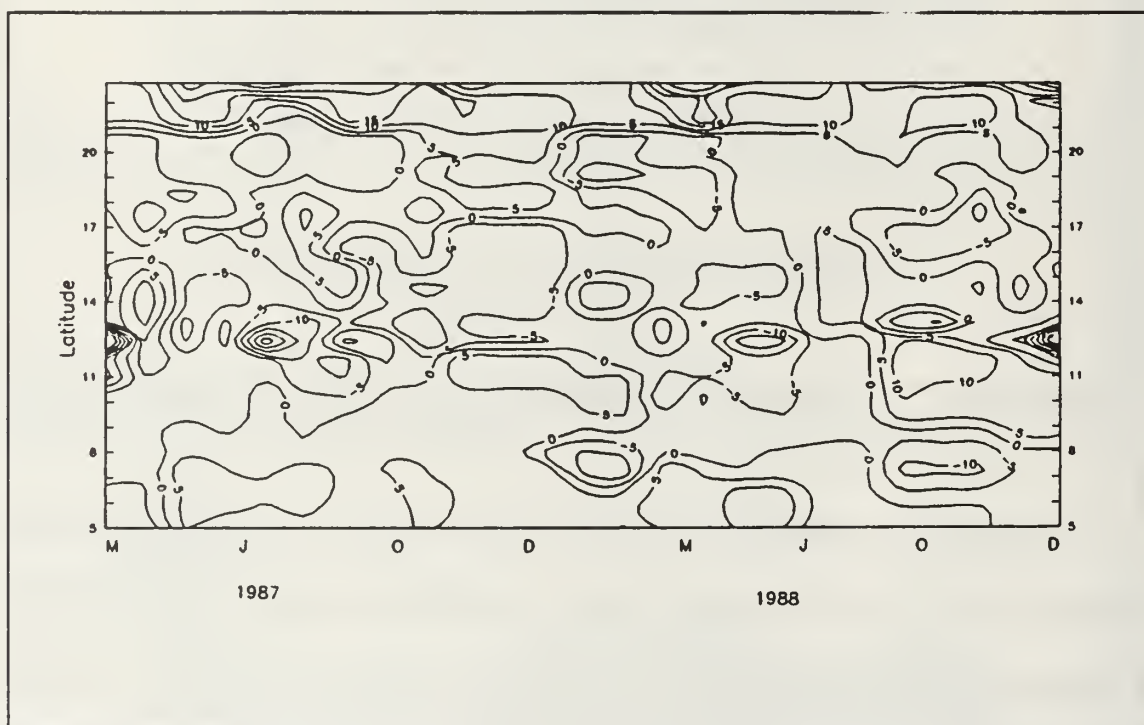


Figure 23 Time series of the height anomalies for Orbit B in Figure 6.

Finally the root mean square variability was calculated for each grided point along the whole basin and contoured as shown in Fig. 24. Maximum values were found south of Hispaniola in the Colombian Basin where the meandering and

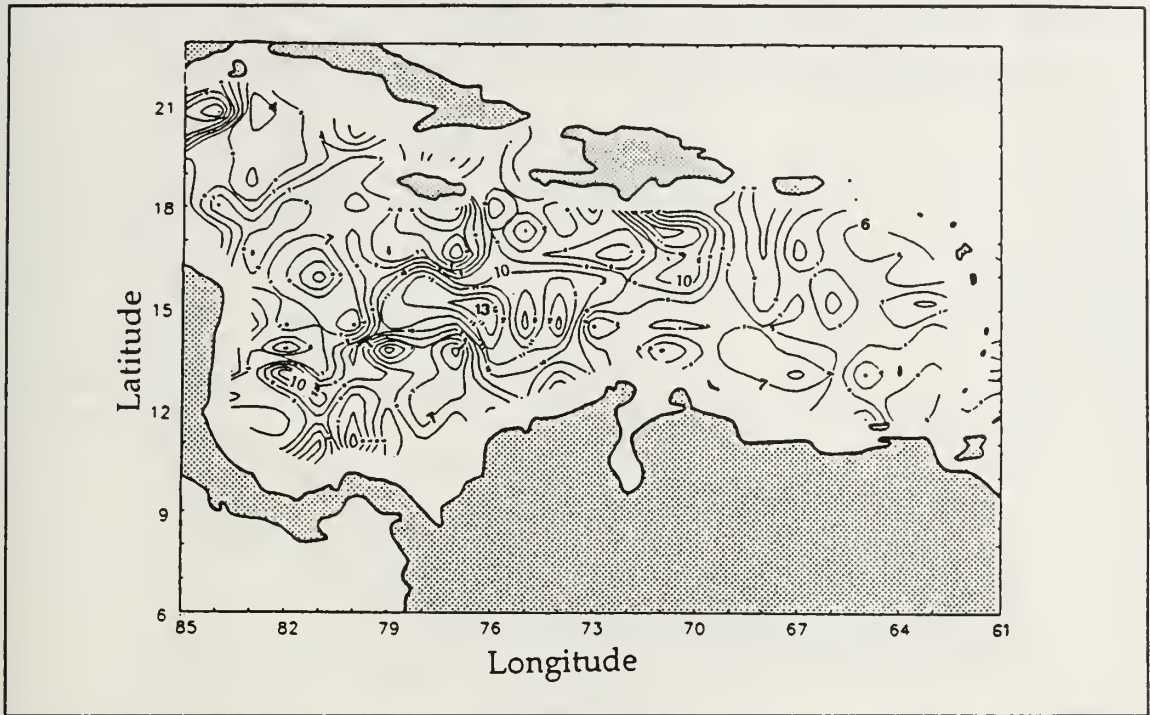


Figure 24 Root Mean Square variability during 1987-88 (cm). contour interval is 1.cm.

eddy activity were most intense and in the southwestern Caribbean where the quasi-permanent cyclonic eddy movement was detected. This provides additional evidence of eddies in the region.

B. WIND ANALYSIS

Time series of the wind speed at various locations in the Caribbean Sea, Fig. 25 were made in order to observe their variability. The wind speed shows a bimodal seasonal variation along the whole basin. In general, the wind is strong in winter between November and March, followed by a rapid decrease in wind speed between March and May. There is an increase in the intensity during June and September, known as the "Veranillo", followed by a decrease in intensity until

November when the windy season begins again. The wind is always intense

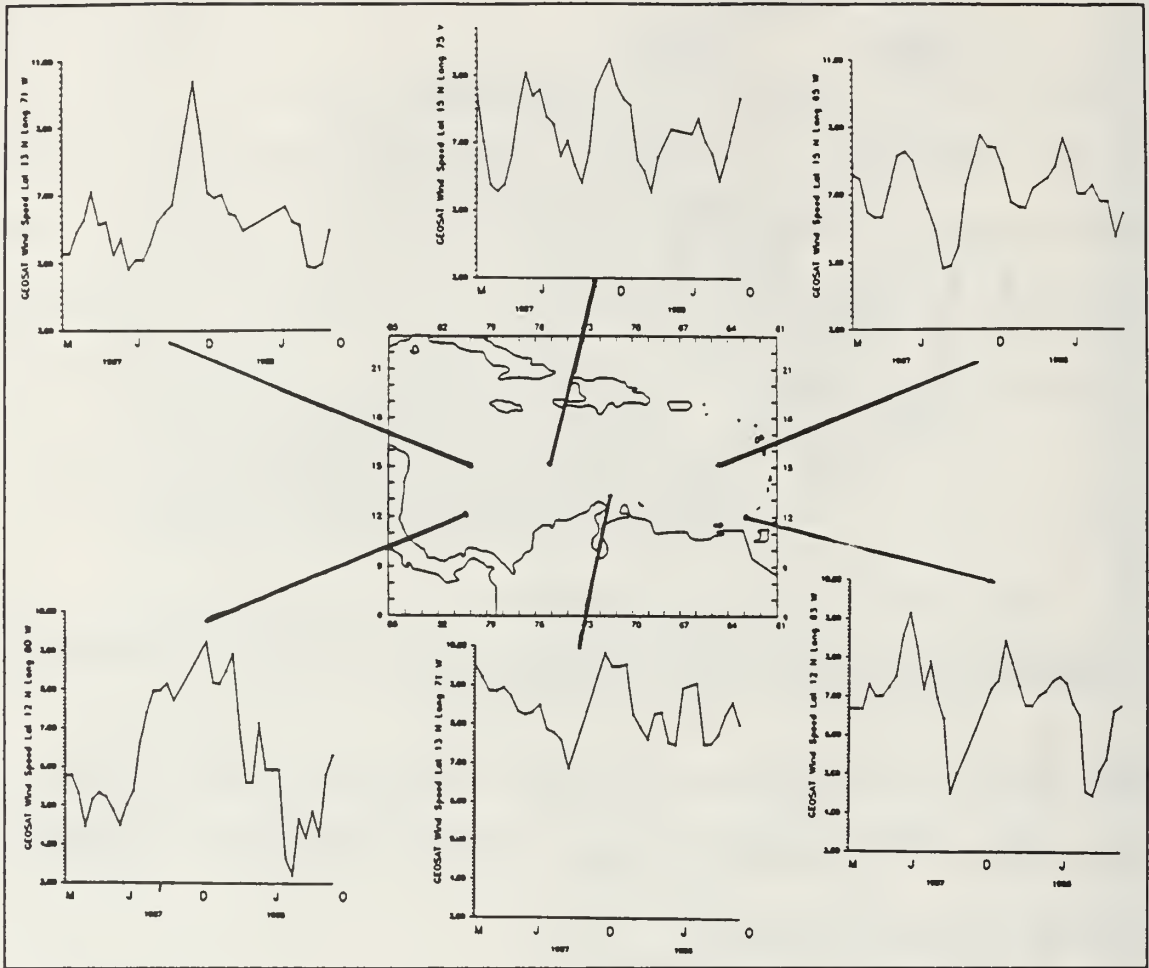


Figure 25 Wind Speed in the Caribbean during 1987-88.

(above 7 m/s) north of the South American coast in the center of the basin, where upwelling has been reported by several works mentioned earlier. The stations in the western part do not show high winds during the "Veranillo".

Seasonal averaging of the wind speed was made for these periods. The wind speed during March-May of 1987, Fig. 26, shows maximum values in the center of the Caribbean with winds above 7 m/s dominating the center and eastern part

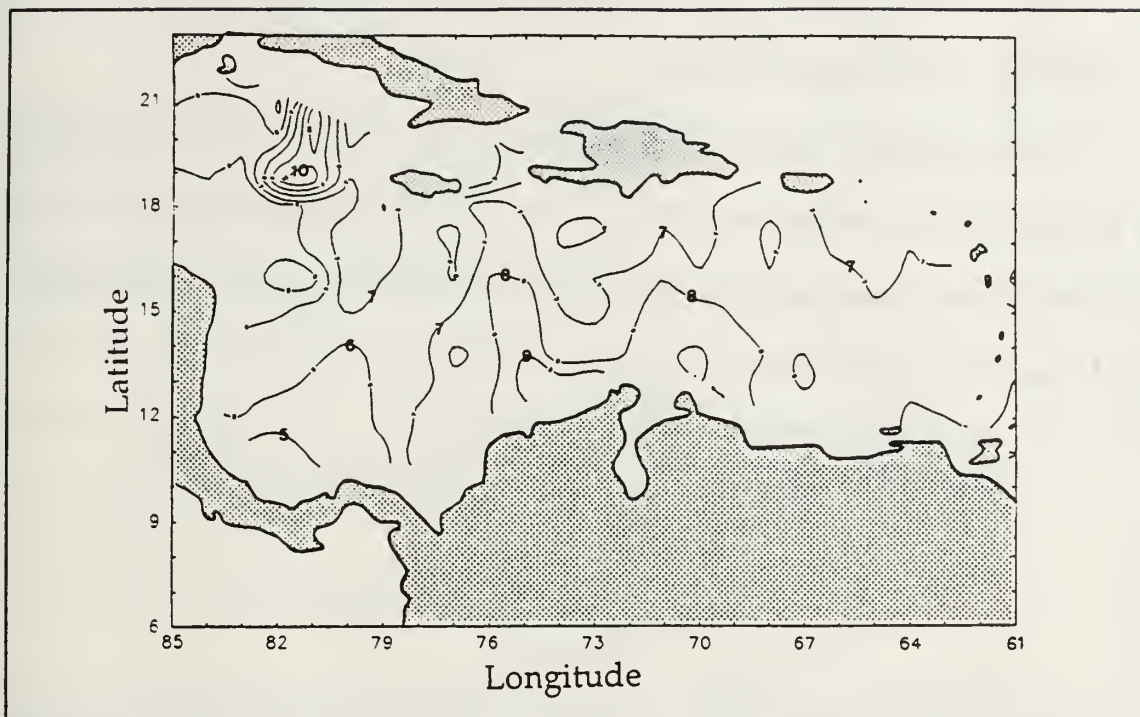


Figure 26 Wind Speed March-May 1987 (contour interval 1 m/s)

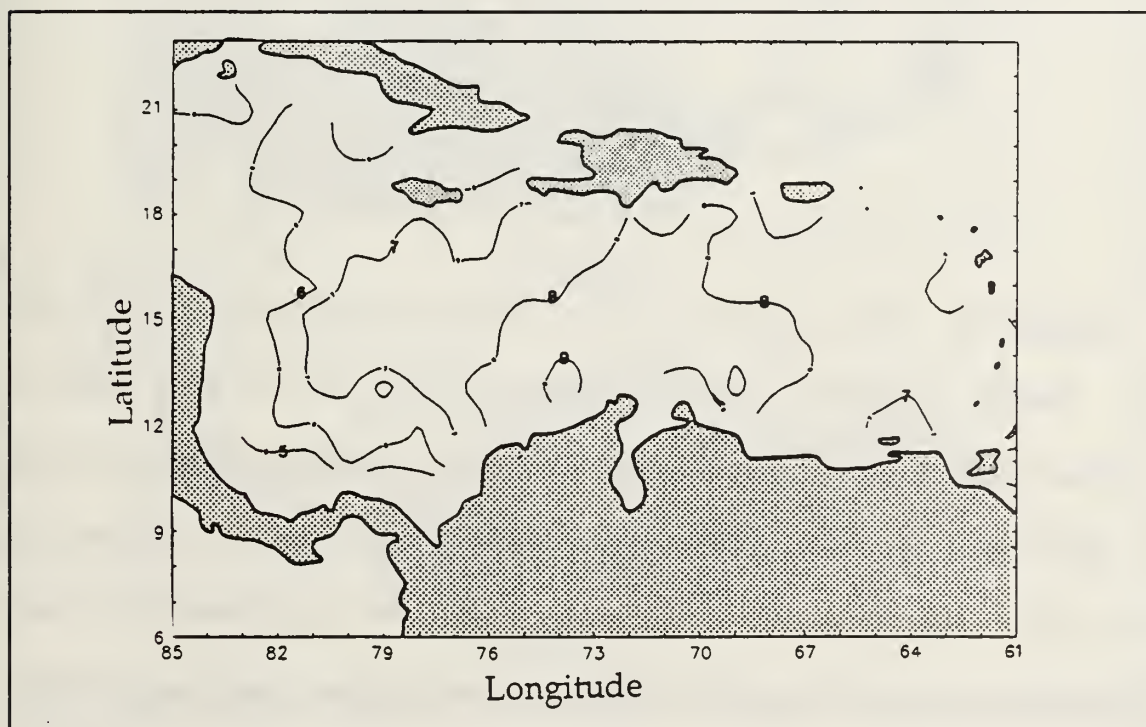


Figure 27 Wind Speed May-Sept 1987 (contour interval 1 m/s)

of the basin. Wind speed is somewhat less in the western part and there is a localized maximum south of Cuba.

The wind speed during May-September of 1987 (Fig. 27), shows an increase in the field in the whole basin to over 7 m/s dominating over most of the Caribbean. The central Caribbean has winds of 8 m/s and maximum values above 9 m/s occur near the South-American coast.

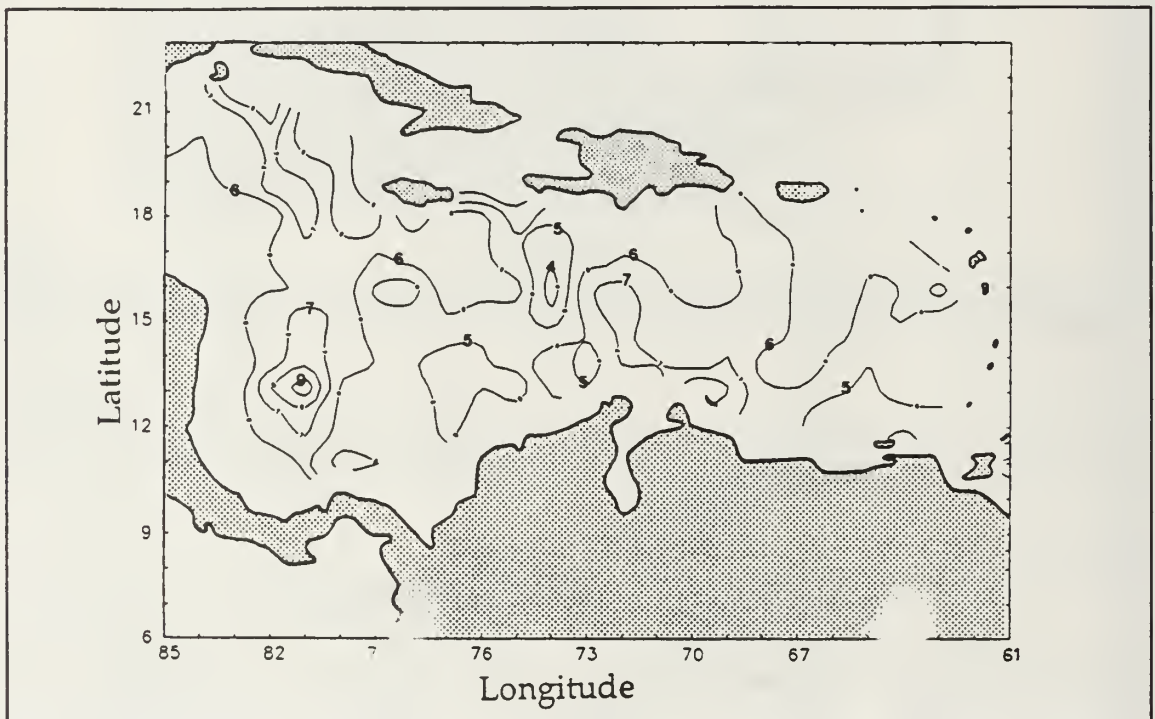


Figure 28 Wind Speed Sept-Nov 1987 (contour interval 1 m/s)

During September and November 1987, Fig. 28, the wind speed has diminished in the central and eastern Caribbean but a local maximum is found in the western part. The windy season during November 1987 to March 1988, (Fig. 29), is characterized by a general increase in the wind speed in the central and eastern part with maximum values greater than 9 m/s near the Colombian

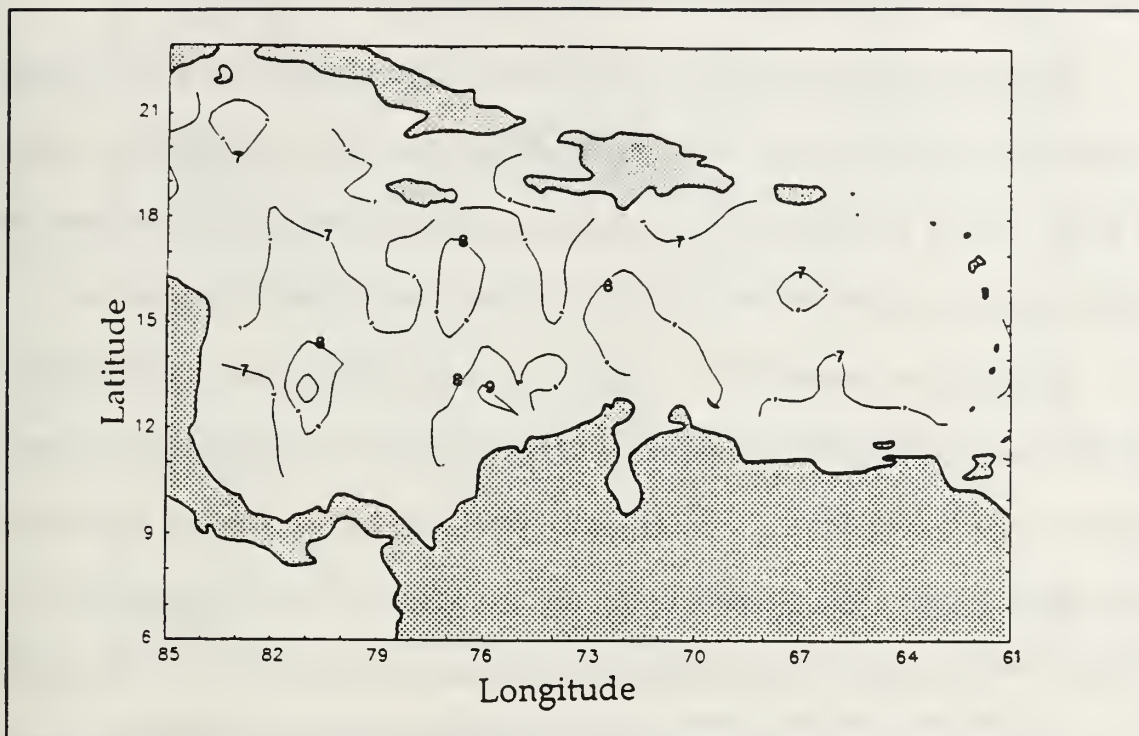


Figure 29 Wind Speed during November/87 - March/88 (m/s)

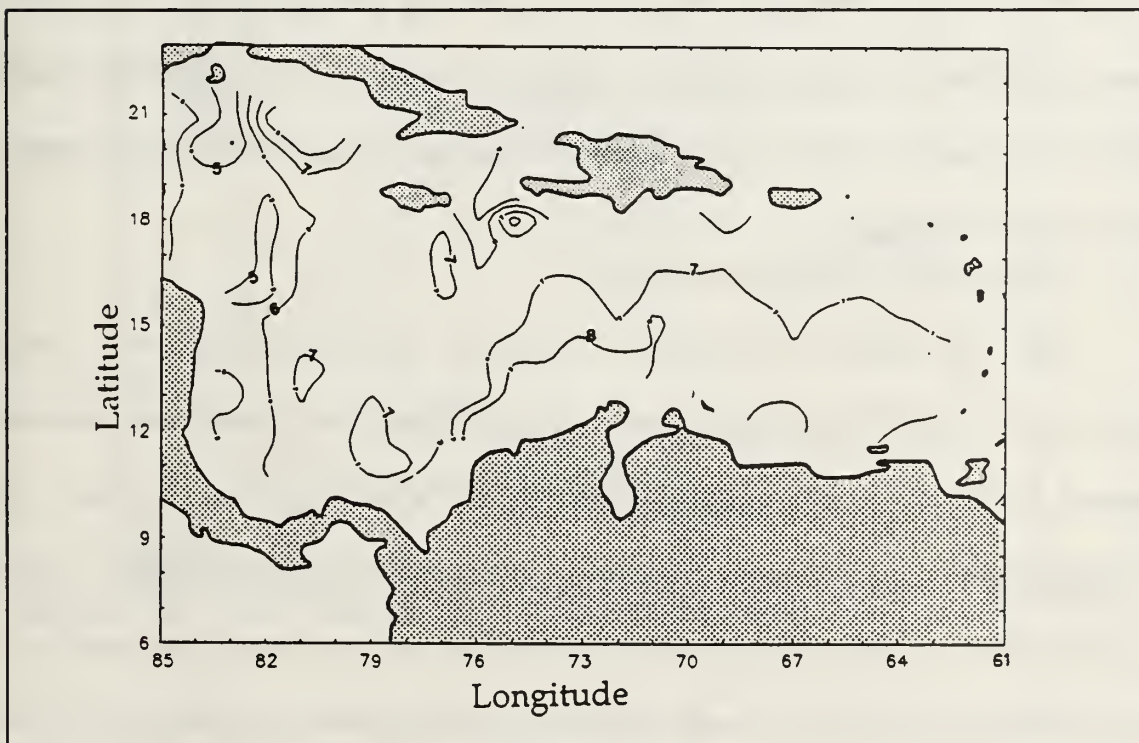


Figure 30 Wind Speed Mar-June 1988 (contour interval 1 m/s)

coast. The western part shows a significantly lower wind speeds.

The final data period (March - June 1988, Fig. 30) shows the wind speed exhibiting the same features as in the same season of 1987 with stronger winds of about 7 m/s in the central and eastern part, maximum values toward the South-American coast and slower winds in the western part of the basin.

The hurricane season in the Caribbean occurs during fall in the Northern Hemisphere. During 1987 the season was benign with two hurricanes just barely entering the basin, Fig. 31 (from Case 1988). However, during 1988, three hurricanes crossed the Caribbean as can be seen in Fig. 32 (from Gross et al.,1989). The average wind speed map derived from GEOSAT for this season was contaminated by the presence of localized anomalies due to Hurricane "Gilbert" as it was crossed by the GEOSAT satellite west of Jamaica (Fig. 33). A similar anomaly occurred during September - November 1988 apparently due to Hurricane "Keith" which contaminated the seasonal average in the southwestern part of the Caribbean.

C. DISCUSSION OF THE RESULTS

Both sequences of mesoscale variability showing anticyclonic eddies traveling through the Caribbean Sea begin in the season of lower wind intensity (March to May) of both years. Apparently the wind plays an important role modulating the conditions for the development of mesoscale anomalies. Seasons with relatively strong wind speed and no meridional wind speed gradient across the Caribbean showed a few weak anomalies associated with the Caribbean Current

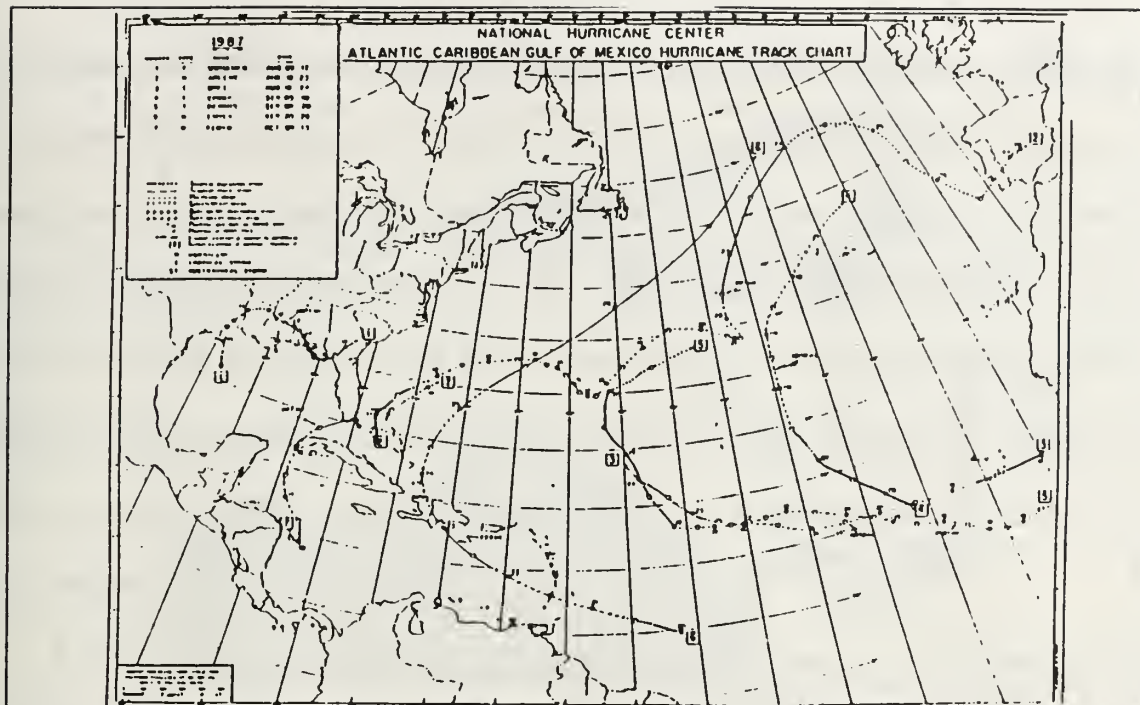


Figure 31 Hurricanes in the Caribbean in 1987 (in Case, 1988)

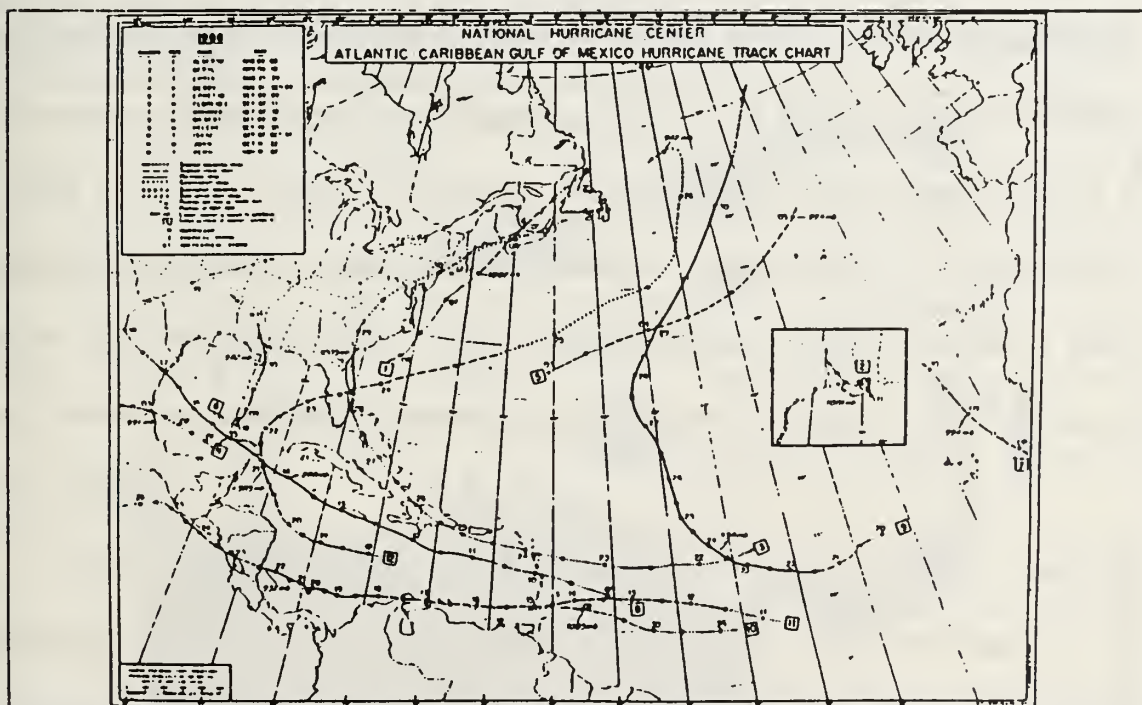


Figure 32 Hurricanes in during 1988 (Gross et al., 1989) 8)

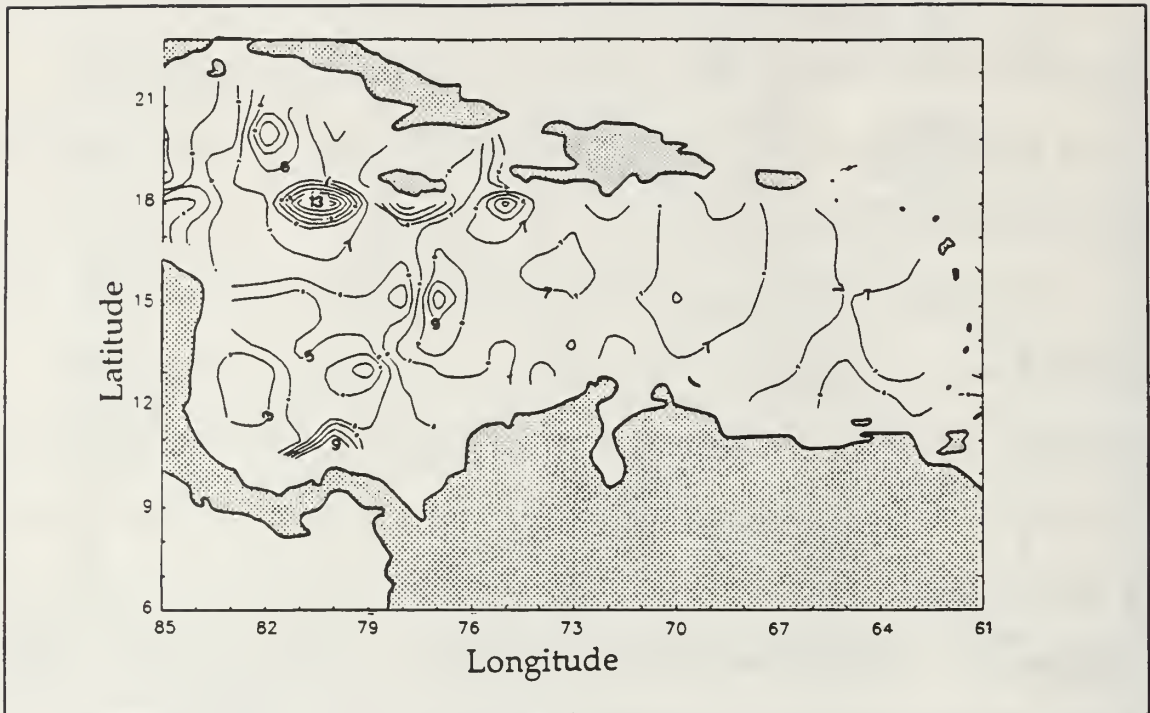


Figure 33 Wind speed Jun-Sep 1988 (contour interval 1 m/s)

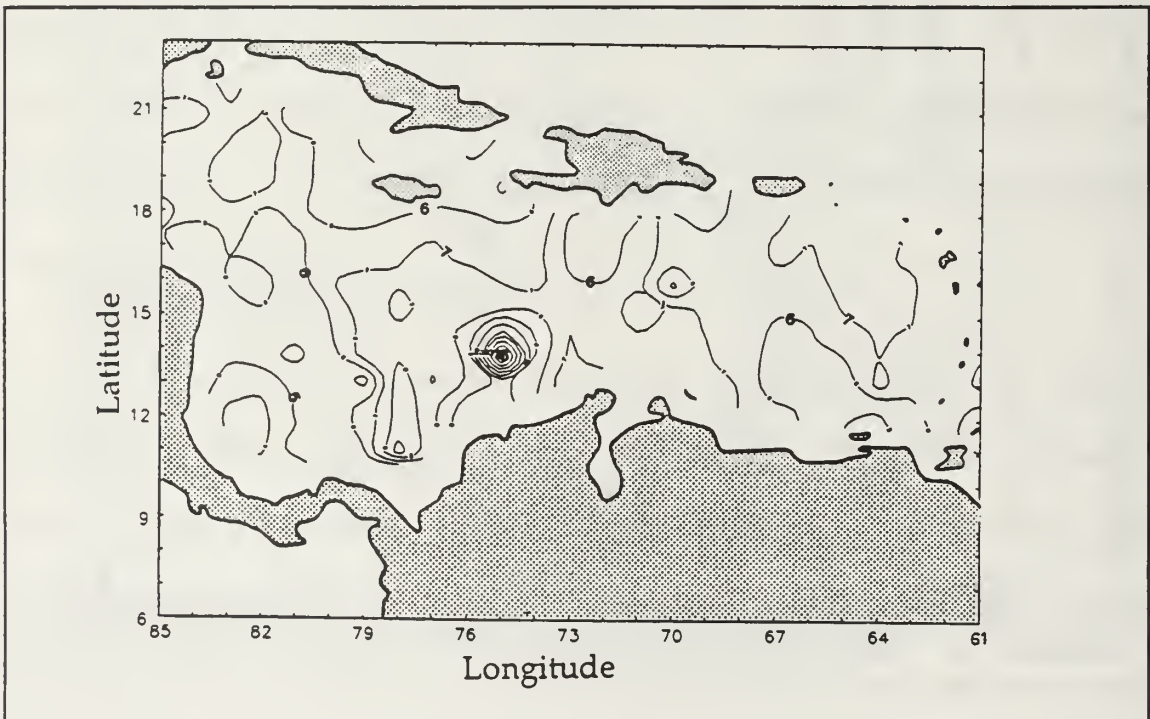


Figure 34 Wind Speed Sept-Nov 1988 (contour interval 1 m/s)

in the east and center part of the Basin, suggesting a stable mean flow. When the wind speed diminished and a meridional wind speed gradient was present, the mean flow becomes less stable and strong ($> +20$ cm) signals appear in the center of the Caribbean suggesting the formation of anticyclonic eddies that can last for more than three months as was the case of the one detected in May-July 1987. Anticyclones associated with the Caribbean Current were modeled by Thompson (pers. commun.,1990) but with dynamic height anomalies not greater than 10 cm with respect to the surroundings.

Relatively strong meanders and eddies were detected in the central part of the Caribbean. This finding agrees with Molinari et al. (1981), however, they suggested that meanders in the region are due to the presence of the Beata Ridge. This seems unlikely as the Beata Ridge is a deep ocean feature (shallowest depth is 3000 m in the central Caribbean). Also the barotropic Rossby radius of deformation at the latitude of the Caribbean is of about 4000 km, significantly larger than the dimensions of the Caribbean Basin itself. The most likely mechanism for generation of the eddies is the seasonal change in the structure of the wind field.

The southwestern part of the Caribbean does not lie in the main axis of the Caribbean Current. The most interesting mesoscale feature in this area was the cyclonic eddy located near the San Andres Archipelago. This quasi-permanent feature appeared at various times during the study period. The data processing done to remove the geoid may have removed part of the dynamic height

associated with this feature. It was detected by this study because it does apparently drift slightly in the vicinity of the San Andres Archipelago. It is known that this is the part of the Caribbean that is most affected by the presence and movement of the ITCZ .

This work showed how the wind speed field changes, but unfortunately there is no information on the direction of the wind in the GEOSAT data. From climatology, the southwestern Caribbean has a wind speed regime which behaves in an opposite fashion with respect to the rest of the Basin. It is stronger during the "non windy" season than the rest of the Caribbean and relatively slower during the "windy" seasons. This fact agrees with the typical characteristics of the ITCZ stated by Elsberry et al., (1985) and Pujos et al. (1986) Due to the fact that GEOSAT data samples the same area every 17 days, the highest frequency that can be resolved is 34 days. The "quasi-monthly" average mean wind speed fields generated here were able to describe the general patterns of this field when no small and intense synoptic events occurred in "the month". However during the hurricane seasons, hurricanes contaminated the mean wind field even with the extensive averaging procedure used here. This indicates a strong limitation for the use of the wind field generated by GEOSAT. At mid-latitudes, where frequent mesoscale weather features exist during all seasons, it may not be possible to generate useful climatic wind fields.

V. CONCLUSIONS

This investigation has produced maps of oceanic mesoscale variability in the Caribbean Sea during several seasons based on two years of GEOSAT altimeter data. The method used tracks mesoscale features as they evolve through the Basin.

Anticyclonic eddies which formed in the center of the Basin during the non windy season (March - May) were detected in both years with height signatures that reached +30 cm in 1987 and +20 cm in 1988. These eddies moved toward the west, apparently displaced by the Caribbean Current. No eddies associated with the Caribbean Current were apparent during the other seasons.

A cyclonic eddy in the San Andres Archipelago area was detected frequently during both years of study, this eddy seems to be a quasi-permanent feature of the Western Caribbean. This eddy has been predicted by models, e.g. Gordon (1990) and Thompson (1990).

The seasonal wind field as detected by GEOSAT data showed periodicity that agrees with previous studies, e.g. Pujos et al.(1986). Averaged seasonal wind speed maps derived from GEOSAT data showed permanent maximum values in the central Caribbean near the South-American coast. During the "rainy" seasons a strong gradient in the wind field occurs in the center of the basin together with a general diminishing in the intensity of the easterlies.

The relaxation of the wind after the windy season coincided with the formation of the anticyclones, suggesting that the wind field influences eddy formation.

Anomalies in the averaged wind field were produced by the sub-resolution of strong synoptic events (hurricanes) which contaminate the averaging technique.

LIST OF REFERENCES

- Anderson, D.L.T., and R.A. Corry, Seasonal transport variations in the Florida Straits: A Model study. *Journal of Physical Oceanography*, V.15, 773-786, 1985.
- Aguilera, J., and C. Andrade (1989). Condiciones oceanográficas en el Archipielago de San Andres con base en los Cruceros OCEANO. submitted to the *Boletin Cientifico CIOH*, January 1990.
- Atwood, D.K., P.N. Froelich, M.E.Q. Pilson, M.J. Barcelona and J.L. Vilen, Deep silicate content as evidence of renewal processes in the Venezuela Basin, Caribbean Sea. *Deep-Sea Research*, V.26a, 1179-1184, 1979.
- Case, R.A., North Atlantic Tropical Cyclones, 1987. *Marines Weather Log*, Winter 1988, V.32 (1): 11-16, 1988.
- Chelton, D.B., M.G. Schlax, D.L. Witter and J.G. Richman, GEOSAT Altimeter observations of the surface circulation of the southern ocean. *Journal of Geophysical Research*, V.95 (C10), 17877-17903, October 1990.
- Cheney, R.E., B.C. Douglas, R.W. Agreen, L.L. Miller, D.L. Porter, GEOSAT Altimeter Geophysical Data Record (GDR) User Handbook. NOAA Technical Memo. NOS-NGS-46, 1987.
- Corredor, J.E., Phytoplankton response to low level nutrient enrichment through upwelling in the Colombian Caribbean Sea. *Deep-Sea Research*, V.26a, 731-741, 1979.

- Dietrich, G., Das Amerikanische Mittelmeer. Ges. Erd., 1939.
- Douglas, B.C., R.E. Cheney, and R.W. Agreen, Eddy energy of the Northwest Atlantic and Gulf of Mexico determined from GEOS-3 altimetry. Journal of Geophysical Research, V.88 (C14): 9595-9603, 1983.
- Dobson, E., F. Monaldo, J. Goldhirsh and J. Wilkerson, Validation of GEOSAT Altimeter-derived wind speeds and significant wave heights using buoy data. Johns Hopkins APL Technical Digest. V.8,(7) 222-233, 1987.
- Elsberry, R.L., W.M. Frank, G.J. Holland, J.D. Jarell, R.S. Southern, A global view in tropical cyclones. Summary of material prepared for the International Workshop on Tropical Cyclones, Bangkok, Thailand, 1985.
- Fajardo, G.E., Surgencia costera en las proximidades de la peninsula colombiana de la Guajira. Boletín Científico CIOH, V.1, 7-19, 1979.
- Froelich, Jr. P.N. and D.K. Atwood, New evidence for sporadic renewal of Venezuela Basin Water. Deep Sea Research, Deep Sea Research, V.21, 969-975, 1974.
- Froelich, Jr. P.N., D. Atwood, and G.S. Giese, Influence of the Amazon River discharge on surface salinity and dissolved silicate concentration in the Caribbean Sea. Deep-Sea Research, V.25, 735-744, 1978.
- Gordon, A., Circulation of the Caribbean Sea. Journal of Geophysical Research, V.72, 6207-6233, December 1967.
- Gross, J.M., and M.B. Lawrence, North Atlantic Tropical Cyclones, 1988, Mariners Weather Log, Spring 1989, V.33 (2): 8-14, 1989.

- Hansen, D.V. and R.L. Molinari, Deep currents in the Yucatan Strait, *Journal of Geophysical Research*, V.84 (C1), 359-362, January 1979.
- Hansen, D.V. and G.A. Maul, Anticyclonic current rings in the Eastern Tropical Pacific Ocean. Submitted to the *Journal of Geophysical Research*, 1990.
- Hydaka, K., Computation of the wind stress over the oceans, *Rec. Oceanographic Works Japan* 77-123, 1958.
- Kjerfve, B., Tides in the Caribbean Sea. *Journal of Geophysical Research*, V.86 (C5) 4243-4247, May 1981.
- Leben, R.R., G.H. Born, J.D. Thompson and C.A. Fox, Mean Sea Surface and variability of the Gulf of Mexico using GEOSAT Alimetry data. *Journal of Geophysical Research*, V.95 (C3), 3025-3032, March 1990.
- Lilly, J.E., The performance of the GEOSAT altimeter during a period of increased solar activity. Work presented to the Advanced Remote Sensing Class, Naval Postgraduate School, 1989.
- Marsh, J.G., R.E. Cheney, J.J. McCarthy, and T.V. Martin, Regional mean sea surfaces based on GEOS-3 and SEASAT altimeter data. *Mar. Geod.*, V.8(1-4): 385-402, 1984.
- Maul, G.A., Oceanic circulation in the Caribbean Sea and Adjacent Regions: An Intergubernamental oceanographic commission proposal to the European Space Agency for ERS-1 science, application and validation. 22p., 1988.

- Maul, G.A., J.R. Proni, M. Bushnell and J.L. Mitchell, Oceanic dynamic height anomaly from GEOSAT: A conceptual model for short collinear orbit segments. *Marine Geodesy*, V.12 : 259-285, 1988.
- Mofjeld, H.O. and M. Wimbush, Bottom pressure observations in the Gulf of Mexico and the Caribbean Sea. *Deep Sea Research*, V.24, 987-1004, 1977.
- Molinari, R.L., M. Spillane, I. Brooks, D. Atwood, and C. Duckett, Surface currents in the Caribbean Sea as deduced from Lagrangian observations. *Journal of Geophysical Research*, V.86 (C7), 6537-6542, July 1981.
- Montgomery, R.B., Observation of vertical humidity distribution above the ocean surface and their relation to evaporation, *Paper Physical Oceanography and Meteorology*, 7, 30 pp. 1940.
- Morrison, J.M., and W.D. Nowlin Jr., General distribution of water masses within the eastern Caribbean Sea during winter of 1972 and fall of 1973. *Journal of Geophysical Research*, V.87 (C6), 4207-4229, May 1982.
- Munk, W., A critical wind speed for air-sea boundary process. *Journal of Marine Research*, V.6 203-218, 1947.
- Parr, A.E., A contribution to the hydrography of the Caribbean and Cayman Seas. *Bulletin Biml. Oceanography*, Coll.5, art.4, 1-110, 1937.
- Pujos, M., J. Pagliardini, R. Steer, G. Vernet and O. Weber., Influencia de la Contra-corriente norte colombiana para la circulación de las aguas en la plataforma continental : Su acción sobre la dispersión de los efluentes en suspensión del Río Magdalena. *Bol. Científico CIOH*, V.6, 3-15, January 1986.

- Richards, F.A. and R.F. Vaccaro, The Cariaco Trench, an anaerobic basin in the Caribbean Sea. Deep Sea Research Bulletin, V.3 (3), 214-228, 1956.
- Richards, F.A., Some chemical and hydrographic observations along the north coast of South America. I. Cabo Tres Puntas to Curacao including the Cariaco Trench and the Gulf of Cariaco. Deep-Sea Research, V.7 (3): 163-182, 1960.
- Roemmich, D., Circulation of the Caribbean Sea: A well-resolved inverse problem. Journal of Geophysical Research, V.86 (C9), 7993-8005, September 1981.
- Sadler, J.S., On the origin of tropical vortices. Proceedings Working Panel on Tropical Dynamical Meteorology. NWRP 12-1167-132, Navy Weather Research Facility: 39-76, 1967.
- Stommel, H., A survey of ocean current theory, Deep-Sea Research, V.4: 149-184, 1957.
- Shuhy, J.L., M.R. Grunes, E.A. Uliana, and L.W. Choy, Comparison of GEOSAT and Ground-truth wind and wave observations: Preliminary results. Johns Hopkins APL Technical Digest, 8 (2): 219-221, 1987.
- Sturges, W., Water characteristics of the Caribbean Sea. Journal Marine Research, V.23 (2): 147-162, 1965.
- Tournadre, J. and R. Ezraty , Local climatology of wind and sea state by means of satellite radar altimeter measurements. Journal of Geophysical Research. V.95 (C10): 18255-18268, October 1990.

- Worthington L.V., A new theory of Caribbean bottom-water formation. Deep Sea Research, V.3: 82-87, 1955.
- Worthington L.V., Recent oceanographic measurements in the Caribbean Sea. Deep Sea Research, V.13: 731-739, 1966.
- Wust, G., On the stratification and circulation of the cold water sphere of the Antillean-Caribbean Sea. Deep Sea Research, V.10: 165-187, 1963.
- Wust, G., Stratification and Circulation in the Antillean-Caribbean Basins. Part I., Spreading and mixing of the Water Types with an Oceanographic Atlas. Columbia University Press. New York, 201pp. 1964.
- Zlotnicki, V., A. Hayashi and L. Fu., The JPL-Oceans-8902 version of GEOSAT Altimetry data. JPL Technical Report D-6939, 47pp., June 1989.

INITIAL DISTRIBUTION LIST

	No. Copies
1. Library, Code 0142 Naval Postgraduate School Monterey, CA 93943-5100	2
2. Chairman (Code Oc/Co) Department of Oceanography Naval Postgraduate School Monterey, CA 93943-5000	1
3. Chairman (Code Me/He) Department of Meteorology Naval Postgraduate School Monterey, CA 93943-5000	1
4. Professor Jeffrey Nystuen (Code Oc/Ny) Department of Oceanography Naval Postgraduate School Monterey, CA 93943-5000	3
5. Professor Carlyle Wash (Code Me/Wa) Department of Meteorology Naval Postgraduate School Monterey, CA 93943-5000	1
6. Sr. Director Escuela Naval "ALMIRANTE PADILLA" Cartagena, Colombia.	1
7. Sr. Director Centro de Investigaciones Navales A.A. 982 Cartagena, Colombia.	1
8. Defense Technical Information Center Cameron Station Alexandria, VA 22304-6145	2

Thesis
A4892 Andrade Amaya
c.1 Mesoscale variability

ID:32768000111702
A4892
Mesoscale variability
Andrade Amaya

Thesis
A4892 Andrade Amaya
c.1 Mesoscale variability
of the Caribbean Sea
from GEOSAT.



DUDLEY KNOX LIBRARY



3 2768 00011170 2